

Elemental analysis of atmospheric particulate matter samples with Ion Beam Analysis techniques

Massimo Chiari

chiari@fi.infn.it

INFN division of Florence

Via G. Sansone 1, 50019 Sesto Fiorentino

ITALY

Table of contents

Table of contents.....	1
List of Figures.....	
List of Tables.....	
Abbreviations.....	
1. Introduction to Ion Beam Analysis (IBA) techniques.....	
2. Particle Induced X-ray Emission (PIXE): basic physical principles.....	
2.1 Advantages and limitations of PIXE analysis of APM samples.....	
2.2 Analysis of PIXE spectra.....	
2.2.1 <i>Quantitative analysis in thin target approximation</i>	
2.2.2 <i>Detection limits</i>	
2.2.3 <i>Uncertainty budget</i>	
3. Particle Induced Gamma Ray Emission (PIGE): basic physical principles.....	
3.1 Advantages and limitations of PIGE analysis of APM samples.....	
3.2 Analysis of PIGE spectra.....	
3.2.1 <i>Quantitative analysis in thin target approximation</i>	
3.2.2 <i>Detection limits</i>	
3.2.3 <i>Uncertainty budget</i>	
4. Elastic scattering techniques: basic physical principles.....	
4.1 Advantages and limitations of EBS and PESA analysis of APM samples.....	
4.2 Analysis of EBS and PESA spectra.....	
4.2.1 <i>Quantitative analysis in thin target approximation</i>	
4.2.2 <i>Detection limits</i>	
4.2.3 <i>Uncertainty budget</i>	
5. Feasibility of IBA measurements of APM samples with ambient pressure set-ups.....	
6. Bibliography and references.....	
Appendix A.....	
Appendix B.....	
Appendix C.....	

List of Figures

Figure 1.1. Schematic representation of the IBA techniques applied to the analysis of an aerosol sample using a proton beam, showing the typical detected elements by each different technique.

Figure 1.2. Schematic diagram of a typical IBA set-up used for in-vacuum measurements of APM samples.

Figure 2.1. PIXE spectra of a PM10 sample on Teflon collected in an industrial area. Proton beam energy 2.2 MeV, beam current 6 nA.

Figure 2.2. SDD energy resolution as a function of X-ray count rate, with backscattered proton removal (green line) or not (red line). The lines are drawn as a guide to the eye. The results obtained with a Si(Li) are also shown for comparison. Reproduced from [CA06].

Figure 2.3. PIXE spectra obtained from the measurement of APM samples collected on Nuclepore (in panel a) low-Z elements; in panel b) high-Z elements), where the fitting residues are shown in the bottom of each panel using the GUPIXWIN package.

Figure 2.4. Example of the procedure for determining the elemental concentration by comparison with a reference standard sample, for the case of Na. In panel a) a portion of the PIXE spectrum from a PM2.5 aerosol sample is shown, whereas in panel b) the same energy range of the PIXE spectrum from a NaCl standard ($51.7 \mu\text{g}/\text{cm}^2$) on Mylar is shown. In the latter spectrum the P peak at 2 keV is due to impurities in the Mylar foil.

Figure 2.5. Sensitivity curves for two different Silicon Drift Detectors (different solid angles and entrance windows and absorbers) measured using a set of thin elemental standards supplied from MicroMatter Corp.

Figure 2.6. Measured and interpolated sensitivity curves for an X-ray detector.

Figure 2.7. PIXE spectra of the NIST SRM 2783 “Air Particulate on Filter Media” standard: panel a) low-Z elements; panel b) high-Z elements), The measurement were carried out in an external beam set-up with proton energy (on target) 3 MeV, beam current 14 nA and measurement time 300

s. The X-ray spectrum of the low-Z elements was collected by a SDD, 30 mm² active area, 8 mm Be window, with helium flowing in front of the detector to minimize air absorption, 8 msr subtended solid angle and 135 eV FWHM energy resolution. The X-ray spectrum of the high-Z elements was collected by a SDD 80 mm² active area, 25 mm Be window, with an additional 450 mm Mylar absorber, 180 msr subtended solid angle and 145 eV FWHM energy resolution.

Figure 2.8. Scheme for the measurement of the elemental mass for homogeneous (left picture) and inhomogeneous (right picture) samples. The samples produced by an ISAP1050e sampler are taken as an example.

Figure 2.9. PIXE spectra of a PM10 aerosol sample collected on Nuclepore with a Si(Li) detector for different proton beam energies (listed in keV in the legend). Proton beam current was 15 nA and measurement time 400 s.

Figure 2.10. Normalized PIXE spectra of a PM10 aerosol sample collected on Teflon (blue line) and on a Cellulose Acetate (red line) filters. Proton beam energy 2.85 MeV, beam intensity 5 nA. The increased background in the spectrum region above 10 keV for the measurement on Teflon filter is clearly evident.

Figure 2.11. Example of the procedure for determining the background area for the calculation of MDL for a sample element (Na in the shown case). The PIXE spectrum is the same shown in panel a) of Figure 2.4.

Figure 2.12. PIXE and XRF MDLs, for different elements, for APM samples collected on polycarbonate and Teflon filters. Reproduced from [CA08].

Figure 2.13. Minimum detection limits for: a) Mn and b) Sr in aerosol samples collected on Nuclepore filters as a function of the bombarding proton beam energy.

Figure 2.14. PIXE spectra of a APM sample collected on Teflon filter measured at two proton beam energies. The increase in the continuous background in the X-ray energy region >10 keV for the measurement at 2.85 MeV proton is evident.

Figure 2.15. Figure 2.14. Cross section for the production of 110 keV (blue points) and 197 keV (green points) gamma-rays from $^{19}\text{F}(p,p'\gamma)^{19}\text{F}$ reactions, as a function of proton energy from [JE00], left plot, and [ZA15], right plot. The arrows marks minima in the cross section at the energy of 1.6, 2.2 and 3.0 MeV.

Figure 2.16. Comparison between the MDLs for the various elements detectable with the Si(Li) and with the SDD in a 3.0 MeV proton PIXE measurement on a Teflon filter. For the Si(Li) the measurement lasted 400 s at a beam current 5 nA, while for the SDD lasted only 60 s at a beam current of 50 nA, in order to keep the integrated dose very similar. Reproduced from [LU14].

[...]

Figure 5.1. Pictures of exit nozzles for external beam PIXE set-ups with 500 nm Si_3N_4 (a) and 8 μm Upilex (b) extraction windows.

List of Tables

Table 2.1. Characteristics and performances of X-ray detectors in a 2-detectors PIXE set-up for a balanced detection efficiency over low- and high-energy regions of the X-ray spectrum.

Table 2.2. Comparison of typical characteristics of SDD and Si(Li) devices for X-ray spectroscopy.

Table 2.3. Certified elemental areal concentrations for the NIST SRM 2783 “Air Particulate on Filter Media” standard. For the elements marked with the asterisk (*) the concentrations are reference values only.

Table 2.4. Contents of the GUPIX standard output for the analysis of the PIXE spectrum of the NIST SRM 2783 standard shown in panel a) of Figure 2.7. Some lines were omitted for the sake of clarity.

[...]

Table 5.1. Energy loss and energy straggling of 3 MeV protons through typical extraction windows for ambient-pressure IBA analysis of APM samples.

Table 5.2. Feasibility of IBA analysis of APM samples with broad or collimated beams in external beam or in-vacuum set-ups.

Abbreviations

ADC, Analog-to-Digital Converter

APM, Atmospheric Particulate Matter

EBS, Elastic Backscattering Spectrometry

ED-XRF, Energy-Dispersive X-ray Fluorescence

HPGE, Hyper Pure Germanium Detector

HV, High Voltage

IBA, Ion Beam Analysis

ICP-AES, Inductively Coupled Plasma - Atomic Emission Spectroscopy

ICP-MS, Inductively Coupled Plasma – Mass Spectrometry

LV, Low Volume

MCA, Multichannel Analyser

MDL, Minimum Detection Limit

NRA, Nuclear Reaction Analysis

PESA, Particle Elastic Scattering Analysis

PIGE, Particle Induced Gamma-ray Emission

PIXE, Particle Induced X-ray Emission

PM_{2.5}, Particulate Matter with aerodynamic diameter less than 2.5 µm

PM₁₀, Particulate Matter with aerodynamic diameter less than 10 µm

PM_{10-2.5}, Particulate Matter with aerodynamic diameter between 2.5 and 10 µm

RBS, Rutherford Backscattering Spectrometry

SDD, Silicon Drift Detector

SEB, Secondary Electron Bremsstrahlung

XRF, X-ray Fluorescence

1. Introduction to Ion Beam Analysis (IBA) techniques

Ion Beam Analysis are a suite of analytical techniques that exploit the interactions of rapid (\sim MeV) charged particles with matter to determine the elemental composition and structure of the surface regions of solids (from \sim 0 to 100 micrometers), inferred from measured quantities such as X-ray, gamma-ray and charged particle spectra. IBA are multielemental (from H to U), sensitive to trace elements ($\mu\text{g/g}$), highly quantitative (few %) and traceable, non-destructive techniques so further measurements with other complementary techniques can be carried out. No sample preparation or extraction is necessary, thus reducing the contamination from chemical reagents and possible loss of volatile elements in the sample. For instance, the sample mineralization by concentrated HF prevents the determination by ion coupled plasma (ICP) techniques of Si, one of the most relevant crustal markers.

In atmospheric particulate matter (APM) studies, IBA techniques can produce large databases of elemental concentrations from the low-mass samples coming from air pollution. They provide quantitative source characterisation and identification, extremely useful to environmental pollution agencies and policy makers.

The relevant IBA techniques for APM analysis are Particle Induced X-ray Emission (PIXE), Particle Induced Gamma-ray Emission (PIGE) and the elastic scattering techniques, such as Elastic Backscattering Spectrometry (EBS) and Particle Elastic Scattering Analysis (PESA). PIXE is indeed the most used technique since it detects all elements heavier than Na, including important anthropogenic elements (S, V, Ni, Cu, Zn, As and Pb) and all the crustal elements (Al, Si, K, Ca, Ti, Mn and Fe). The integration of all techniques, performing the so-called “Total-IBA” measurements [JE12], allows a complete characterization of all sample elements, from H to Pb and heavier.

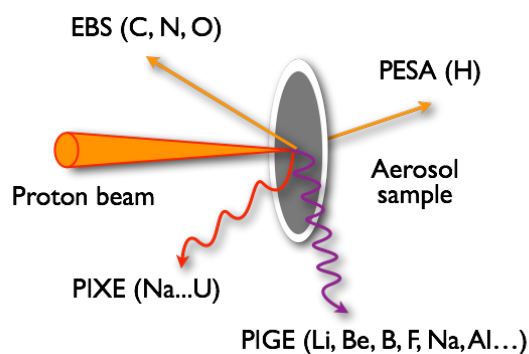


Figure 1.1. Schematic representation of the IBA techniques applied to the analysis of an aerosol sample using a proton beam, showing the typical detected elements by each different technique.

It has to be noted, from an historical point of view, that seminal papers on IBA techniques such as the one by Rubin et al. [RU57] on surface analysis of solids by nuclear scattering (i.e. RBS) and nuclear reactions (i.e. NRA) induced by energetic protons and deuterons showed among the first applications the study of an aerosol deposited over an aluminum filter.

Recommended equipment for total IBA measurements on a APM samples comprises:

- a 2-3 MeV proton beam;
- a light-tight vacuum chamber (pressure 10^{-5} mbar or better) or external beam set-up;
- a target holder, allowing multi-sample mounting and sample changing and movement;
- a Faraday cup for beam charge measurement, with secondary electron suppression, connected to a digital current integrator and to a scaler;
- one or two X-ray detectors, either Silicon Drift Dectors (SDD) or Sil(Li);
- a charged particle detector, either surface barrier or pin diode, placed at any backward scattering angle (135° - 170°);
- (optional) a charged particle detector, either surface barrier or pin diode, placed at any forward scattering angle (30° - 45°);
- a gamma-ray detector, either HPGe or Ge;
- a standard nuclear electronics chain (preamplifier, bias supply, spectroscopy amplifier, ADC and MCA) for each detector;
- a set of thin elemental standards ($Z = 11$ to 82) deposited over light supporting foil (Mylar or Nuclepore);
- a standard reference material, NIST SRM 2783 “Air Particulate on Filter Media”.

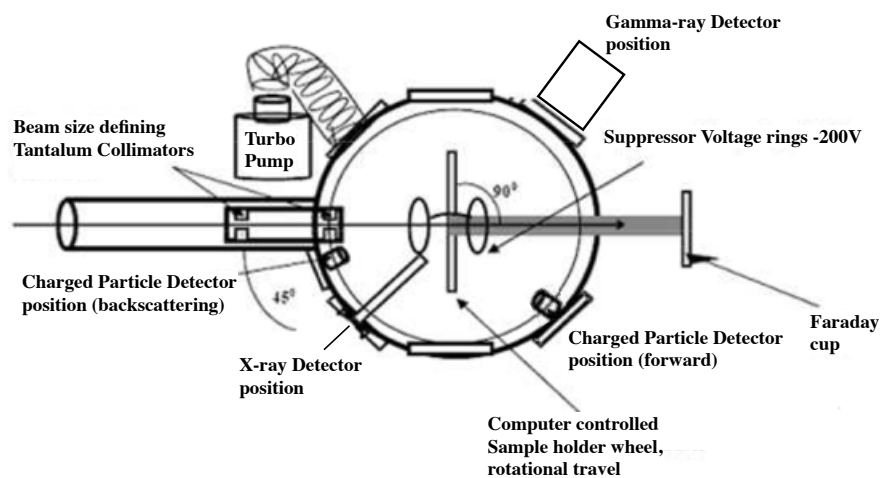


Figure 1.2. Schematic diagram of a typical IBA set-up used for in-vacuum measurements of APM samples.

2. Particle Induced X-ray Emission (PIXE)

Particle Induced X-ray Emission (PIXE, also often referred to as Proton Induced X-ray Emission) is based upon the ejection of inner-shell electrons from target atoms by the energetic incident particle impact, and the spectroscopy of the subsequently emitted X-rays during the electronic deexcitations. Details on the technique can be found in the books listed in Chapter 6. A typical PIXE spectrum (Figure 2.1) consists mainly of the K_α and K_β peaks from the light and medium elements, but L X-rays from heavy elements (such as Lead) are also present.

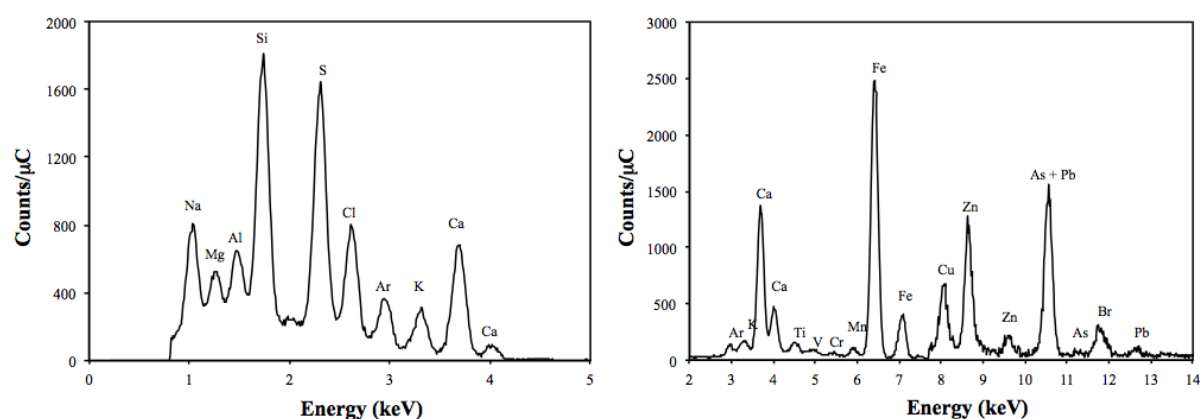


Figure 2.1. PIXE spectra of a PM10 sample on Teflon collected in an industrial area. Proton beam energy 2.2 MeV, beam current 6 nA.

The continuous background radiation for energies typically below 10 keV is Bremsstrahlung radiation emitted by secondary electrons, and there could also be a contribution in the high energy region of the spectrum due to Compton interaction in the X-ray detector active volume from emitted gamma-rays. PIXE analysis involves two basic aspects: assigning observed X-ray peaks (energies) to appropriate elements (element identification) and converting observed X-ray peaks (areas) into elemental concentrations (concentration quantification).

The PIXE technique has been widely used since its birth for the study of the aerosol composition, and for a long time, it has been the dominating technique for its elemental analysis [MA15]. For example, in the PIXE seminal paper by Johansson et al. [JO70], X-ray spectrum of aerosol collected on a carbon foil placed outdoors for 1 day, and then analyzed for 60 min with 2.5 μ A current of 1.5 MeV protons is shown. However, recently, other competitive techniques, such as those based on atomization by induced coupled plasma and detection by atomic emission spectroscopy (ICP-AES) or mass spectrometry (ICP-MS), have been developed. Furthermore

traditional X-ray fluorescence (XRF) systems have been replaced by more efficient modern devices and synchrotron radiation XRF has started to be used for elemental analysis.

PIXE has many advantages for elemental analysis of aerosols: only few minutes (2-10) of bombardment are sufficient to detect elements from Na to Pb, which are markers for specific components or sources of particulate matter, such as marine aerosol (Na, Cl), mineral dust (Al, Si, Ca, Ti, Fe, Sr), sulphates (S), biomass burning or biogenic emissions (K, Zn, Rb), heavy oil combustion (V, Ni), incinerator emissions (K, Zn, Pb), traffic and industrial emissions (Mn, Ni, Cu, Zn, Pb).

The high efficiency of PIXE is very useful when hundreds of samples have to be analyzed, a quite common need in aerosol studies [LU11]. Compared to traditional energy-dispersive XRF (ED-XRF), PIXE offers elemental sensitivities that are typically at least one order of magnitude better and requires much less sample mass, thus allowing the use of samplers with high time and size resolution (i.e. cascade impactors). Another advantage of PIXE over ED-XRF is that it can be complemented with other IBA techniques, as it will be discussed in the following, so that the light elements (H, C, N and O) that make up most of the aerosol mass can be measured as well. However, one should realize that PIXE provides only part of the desired information with regard to the chemical composition; it is also mandatory to perform at least measurements for important ionic species (e.g. ammonium, nitrate), for organic carbon and elemental or black carbon. The use of PIXE data alone (even if proxies coming from IBA techniques are used) may lead to wrong results when applying multivariate receptor modeling for aerosol source apportionment.

Anyway, the PIXE technique can continue to provide an invaluable contribution to air quality studies by giving data for major, minor and trace elements in cases where large numbers of samples are involved. The data for the major elements (S, Na, Cl, Al, Si and Fe) are needed for the assessment of the climatic effect of aerosols, for the estimate of the contributions of important aerosol types (e.g. sea salt and crustal material) and for the achievement of the chemical mass closure. Furthermore, multi-elemental data set as a whole (which comprises data for various anthropogenic tracers) can be used for disentangling the contributions from different source categories by applying multivariate receptor modeling.

2.1 Advantages and limitations of PIXE analysis of APM samples

The main advantage of PIXE analysis are: 1) very fast, high sensitivity, non destructive analytical technique; 2) quantitative analysis is possible; 3) the minimum energy of detected X-rays is about 1 keV (all the elements starting from Na are thus quantifiable simultaneously); 4) it can be performed at ambient pressure (external beam set-up, see Chapter 5).

The main limitations are instead: 1) no information on the organic components of APM samples; 2) no information on chemical states; 3) no information on elemental depth distribution¹; 4) the possible self-absorption of the low energy X-rays inside the aerosol particles/sample can lead to underestimation of the low-Z element concentration (a possible solution can be the simultaneous implementation of PIGE measurements, as discussed in Chapter 3).

Concerning the PIXE detector set-up a better efficiency over all the range of detected elements is achieved if a 2-detectors set-up is adopted, one dedicated to the low-Z element detection, the other to medium-high-Z detection, with features indicated in the table below.

Table 2.1. Characteristics and performances of X-ray detectors in a 2-detectors PIXE set-up for a balanced detection efficiency over low- and high-energy regions of the X-ray spectrum.

Target	X-rays	What is needed	Detector features
Low-Z element	Low energy	Minimum dead layers	Thin entrance window
	High cross sections	Small solid angles	Small active area
Medium- high-Z element	High energy	Efficiency	Large active thickness
	Low cross sections	Large solid angles	Large active area

Note that when using PIXE detectors with a thin entrance window (i.e. 8 μm Be or few μm thick polymeric window) the use of a magnetic proton deflector in front of it is mandatory to prevent any damages in the crystal which could be induced by the beam particles back-scattered from the samples (long-term effects) and to avoid the worsening of the energy resolution (short-term effects), as shown in Figure 2.2.

If only one detector is available then the overall intensity between the high- and the low-energy region of the X-ray spectrum can be effectively balanced using a “funny filter”, i.e. an absorbing foil (typically Mylar or Al) placed in front of the detector with a hole pierced so that a fraction of the X-ray within the detector solid angle is not attenuated. If the funny filter solution is adopted, choose a detector with the largest active area (to increase solid angle) and the thinnest entrance window (to enhance transmission of low-energy X-rays). Since no proton deflector can be inserted the hole of the filter should not be made coaxial, but off-center and the filter should be periodically turned in order to distribute the beam dose and thus the damage over different areas of the solid state X-ray detector.

¹ It has to be noted that in PIXE analysis of layered samples, typical in cultural heritage, for example paint layers, the sequence of layers can be inferred, although at a semi-quantitative level, from the comparison of PIXE spectra collected at various beam energies, performing the so-called “differential” PIXE measurements [FE02].

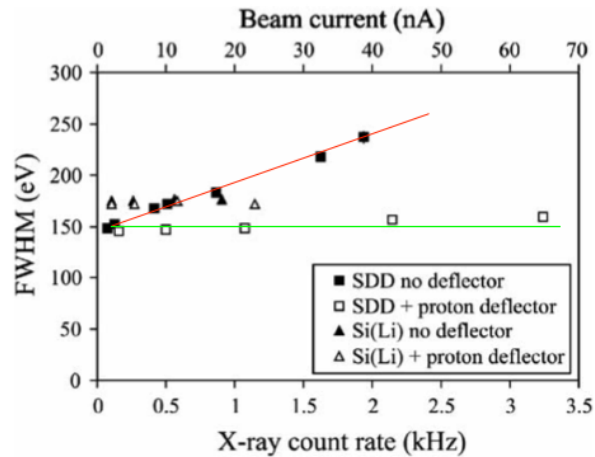


Figure 2.2. SDD energy resolution as a function of X-ray count rate, with backscattered proton removal (green line) or not (red line). The lines are drawn as a guide to the eye. The results obtained with a Si(Li) are also shown for comparison. Reproduced from [CA06].

Nowadays the IBA practitioner has two choices for the X-ray detectors: traditional Si(Li) and Ge(Li) detectors, or the new and unceasingly developed silicon drift detectors (SDDs). First proposed in the early '80s as a position sensitive semiconductor detector for high energy charged particles, based on a novel charge transport scheme where the field responsible for the charge transport is independent of the depletion field [GA84], SDDs are now routinely employed in high-resolution X-ray spectroscopy [LU14,CA15] because of the low capacitance of the collecting electrode (0.5-1 pF/cm²) and the low leakage current (1-2 nA/cm² at room temperature) resulting in improved energy resolution yet at short shaping times, thus allowing also to sustain high count rates. It has to be noted that direct digitisation of the preamplifier signal from the SDD by a digital signal processor (DSP) using digital filtering is emerging as an alternative to conventional analogue pulse electronics, particularly for high counting rates, allowing to reduce dead times. A comparison of the typical performances and characteristics of SDD and Si(Li) devices for X-ray spectroscopy is shown in Table 2.2.

2.2 Quantitative analysis of PIXE spectra

The X-ray spectrum has to be preliminarily calibrated in energy using the position of peaks from simple targets of known composition. For example for the low energy region of the X-ray spectrum a 2-points calibration can be accomplished from the measurement of a thin NaCl standard using the positions of the Na K α peak at 1.04 keV and the Cl K α peak at 2.62 keV. Alternatively encompassing also higher energy spectrum, a 3-points calibration can be accomplished from the measurement of a thin CuSx standard using the positions of the Cu L α peak at 0.93 keV, the S K α peak at 2.31 keV and the Cu K α peak at 8.04 keV. Analysing the NIST SRM 2783 "Air Particulate

on Filter Media” standard the user has even the possibility to choose among four relatively intense X-ray peaks, according to the specific range of detected energies: Si K α peak at 1.74 keV, Fe K α peak at 6.40 keV, Zn K α at 8.63 keV or Pb L α at 10.55 keV.

Table 2.2. Comparison of typical characteristics of commercial SDD and Si(Li) devices for X-ray spectroscopy.

Parameter	SDD	Si(Li)
Active area	7-150 mm ²	10-100 mm ²
Thickness	450 μ m	3-5 mm
Cooling	-10/-40 $^{\circ}$ C w/Peltier cells	-195 $^{\circ}$ C w/Liquid Nitrogen
Shaping time	0.5-1 μ s	6 μ s
Sustainable count-rate	100-200 kHz	5 kHz
Energy resolution (@Mn K α)	130-160 eV	170-200 eV

Spectrum deconvolution is mandatory for obtaining net peak intensities required for the next quantification step. The most used PIXE spectra analysis code for peak fitting and background subtraction is the Guelph PIXE software package, GUPIXWIN (<http://pixe.physics.uoguelph.ca/gupix/main/>) [CA10, IA03]. In Appendix C some practical hints on how to apply GUPIXWIN for the analysis of APM samples (in order to obtain values for peak areas, uncertainties and limits of detection) will be illustrated, whereas in Table 2.4 the example of the information contained in the GUPIX standard output is shown.

Aerosol samples can be considered thin-target samples, so that proton energy loss and X-ray attenuation are negligible, and the so called “matrix effects” drop out. Thus there is a direct linear relationship between the X-ray yield Y_Z and the areal concentration $(\rho t)_Z$ of the element Z , as described in the following equation:

$$Y_Z = \eta_Z \cdot Q \cdot (\rho t)_Z \quad (2.1)$$

where $\eta_Z = (1/e)(N_A/A) \cdot \sigma(E)_Z \cdot (\alpha_Z \cdot \varepsilon_Z \cdot \Delta\Omega/4\pi)$ is a sensitivity factor, i.e. X-ray yield per unit charge per unit areal density for element Z , including in its definition the electron charge (e), the avogadro Number (N_A), the atomic mass of the element (A), the X-ray emission cross section at the beam energy E ($\sigma(E)_Z$), the detector intrinsic efficiency at the characteristic X-ray energy (ε_Z), the solid angle subtend by the detector ($\Delta\Omega$) and the transmission through any absorbers present (α_Z).

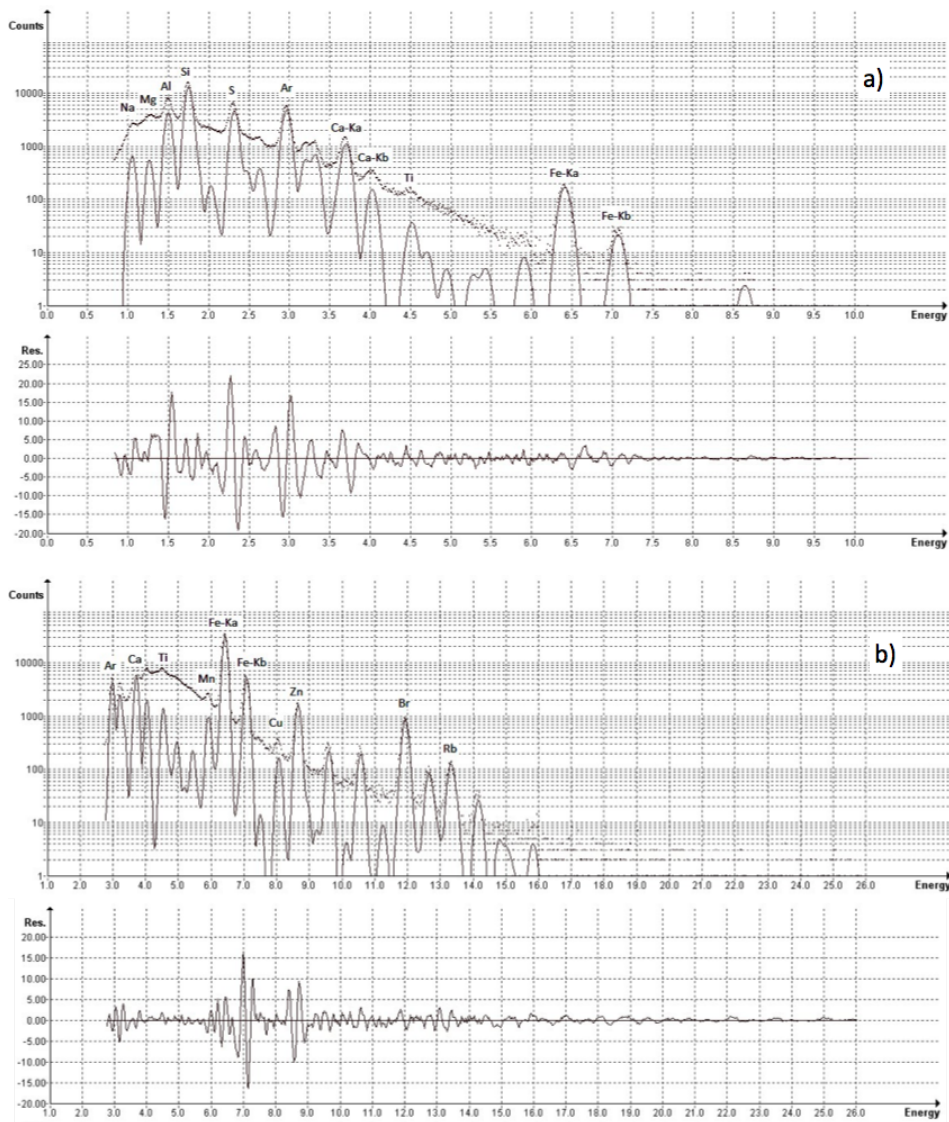


Figure 2.3. PIXE spectra obtained from the measurement of APM sample collected on Nuclepore (in panel a) low-Z elements; in panel b) high-Z elements), where the fitting residues are shown in the bottom of each panel using the GUPIXWIN package.

It is useful to stress that, to estimate the maximum effective energy loss in an aerosol sample, it is essential to take into account the single aerosol particles: for instance, for a 3 MeV proton beam, assuming a density of 2.5 g/cm^3 for the aerosol particles, the maximum energy loss is about 30 keV for an aerosol particle in the “fine mode” (PM2.5, aerodynamic diameter $<2.5 \mu\text{m}$) and it can reach 120 keV for particles in the “coarse mode” (PM2.5-10, aerodynamic diameter between 2.5 and 10 μm). If the energy loss would be computed for the average thickness of a normally loaded filter (about $100 \mu\text{g/cm}^2$), i.e. if the deposit on filters is considered a uniform film, it would not exceed 10 keV.

2.2.1 Quantitative analysis in thin target approximation

In the thin target approximation, quantitative results on elemental concentrations are obtained by comparing the X-ray yield (i.e. counts/ μC) of the sample with the yield of a standard of known concentration, analysed under the same irradiation conditions (geometry, beam energy). In this way the reliance on databases for ionization cross section and ion stopping power is minimized and the need for absolute calibration of beam charge measurement and for determination of the X-ray detector properties are avoided.

The areal concentration $(\rho t)_{Z,\text{sample}}$ of the element Z in the sample is obtained as:

$$(\rho t)_{Z,\text{sample}} = (\rho t)_{Z,\text{std}} \cdot (A_X(Z)/Q)_{\text{sample}} / (A_X(Z)/Q)_{\text{std}} \quad (2.2)$$

where $(\rho t)_{Z,\text{std}}$ is the areal concentration of the element Z in the standard in $\mu\text{g}/\text{cm}^2$, $(A_X(Z)/Q)_{\text{sample}}$ is the ratio of the net X-ray peak area for the element Z , corrected for the fraction of counts lost due to acquisition dead time and pile-up effects, to the total collected proton beam charge from the measurement on the sample, whereas $(A_X(Z)/Q)_{\text{std}}$ is the ratio of the net X-ray peak area for the element Z , again corrected for the fraction of counts lost due to dead time and pile-up, to the total collected proton beam charge from the measurement on the standard. An example of the calculation of areal concentration for Na is given below, with reference to the PIXE spectra shown in Figure 2.4.

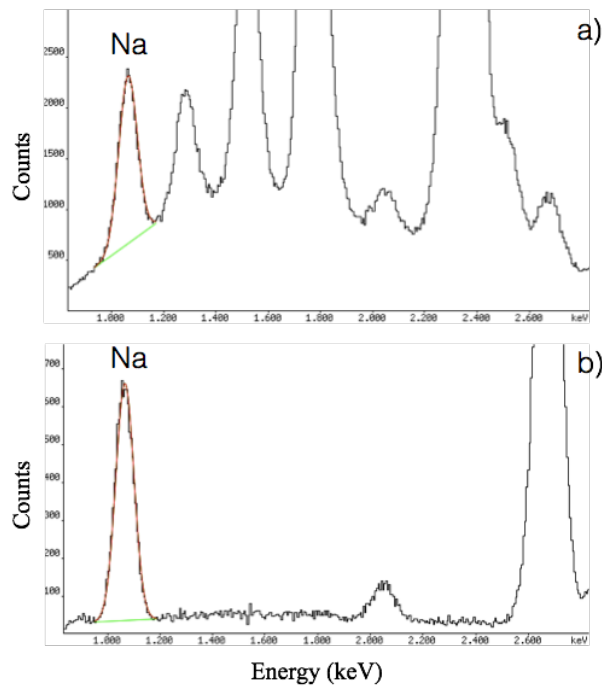


Figure 2.4. Example of the procedure for determining the elemental concentration by comparison with a reference standard sample, for the case of Na. In panel a) a portion of the PIXE spectrum from a PM2.5 aerosol sample is shown, whereas in panel b) the same energy range of the PIXE spectrum from a NaCl standard ($51.7 \mu\text{g}/\text{cm}^2$) on Mylar is shown. In the latter spectrum the P peak at 2 keV is due to impurities in the Mylar foil.

A PM2.5 aerosol sample was analysed with 3 MeV protons and an integrated charge, Q_{sample} , of $5.37 \pm 0.05 \mu\text{C}$. The acquisition dead time resulted 7.7% and there was no pile-up. The area of the Na X-ray peak as obtained by fit and background subtraction of the sample spectrum was 25858 ± 396 counts. This peak area – and consequently the associated uncertainty - had to be corrected for the acquisition dead time multiplying it by $1/(1-0.077)$, in order to obtain a final peak area value, $A_X(\text{Na})_{sample}$, of 28001 ± 429 .

Then, the $51.7 \mu\text{g}/\text{cm}^2$ NaCl standard (uncertainty 5%) was analysed with 3 MeV protons and an integrated charge, Q_{std} , of $0.160 \pm 0.002 \mu\text{C}$. The acquisition dead time resulted 1.5% and again there was no pile-up. The area of the Na X-ray peak as obtained by fit and background subtraction of the standard spectrum was 9581 ± 132 counts. This peak area – and consequently the associated uncertainty - had to be corrected for the acquisition dead time multiplying it by $1/(1-0.015)$, in order to obtain a final peak area value, $A_X(\text{Na})_{std}$, of 9727 ± 134 counts.

The areal density of Na in the NaCl standard is obtained as $(\rho t)_{\text{Na}} = (\rho t)_{\text{NaCl}} \cdot [A_{\text{Na}}/(A_{\text{Na}}+A_{\text{Cl}})]$, that is $(\rho t)_{\text{Na},std} = 51.7 \cdot [23/(23+35.5)] = 20.3 \mu\text{g}/\text{cm}^2$, with an uncertainty of $1.0 \mu\text{g}/\text{cm}^2$.

Finally, applying the formula 2.2 the Na areal density in the PM2.5 aerosol sample resulted $(\rho t)_{\text{Na},sample} = 20.3 \cdot (28001/5.37)/(9727/0.160) = 1.74 \mu\text{g}/\text{cm}^2$. The uncertainty, calculated by propagating with the square-root sums formula the errors on $A_X(\text{Na})_{sample}$, $A_X(\text{Na})_{std}$ and $(\rho t)_{\text{Na},std}$, resulted $0.10 \mu\text{g}/\text{cm}^2$ (5.7%).

Typically a sensitivity curve (expressed in counts/ $\mu\text{C}/(\mu\text{g}/\text{cm}^2)$) is obtained by analysing under the same irradiation conditions mono- or bi- elemental thin standards deposited on Nuclepore or Mylar backing. These standards can be supplied by several manufacturers, such as MicroMatter Corp., choosing thicknesses ranging from 15-25 $\mu\text{g}/\text{cm}^2$ up to 80-100 $\mu\text{g}/\text{cm}^2$.

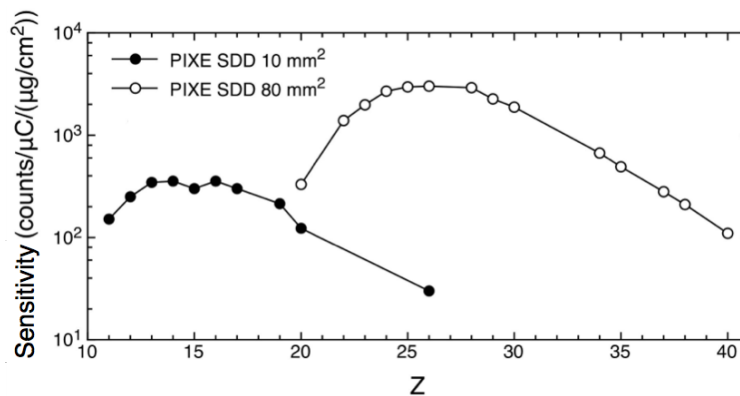


Figure 2.5. Sensitivity curves for two different Silicon Drift Detectors (different solid angles and entrance windows and absorbers) measured using a set of thin elemental standards supplied from MicroMatter Corp.

This measured sensitivity curve subsumes all the physics and all the detector parameters and reduces the analysis to a direct comparison with standards. A suggested set of standards comprising all the main elements of interest for APM analysis is the following: NaCl, MgF₂, Al, SiO, CuS_x, KCl, CaF₂, Ti, V, Cr, Mn, Fe, Ni, Cu, Zn, Ge, Se, CsBr, SrF₂, MoO₃ and Pb, with concentrations in the 40-50 µg/cm² range. In the example discussed above for the Na case, the sensitivity value for Na would have been $\eta_{Na} = 9727/0.160/20.3 = 2995$ counts/µC/(µg/cm²).

In case the sensitivity η_i at the given X-ray energy E_i is not determined experimentally, because the specific elemental standard is not available or its composition and thickness are not reliable (e.g. not stoichiometric standards such as GaP or ZnTe, where the certified thickness is the total for both elements) it can be interpolated from the measured sensitivities η_1 and η_2 at two other X-ray energies E_1 and E_2 (with $E_1 < E_i < E_2$) according to the following formula:

$$\eta_i = e \left[\ln(\eta_1) + \frac{\ln(\eta_1) - \ln(\eta_2)}{E_1 - E_2} \cdot (E_i - E_1) \right] \quad (2.3)$$

based on the assumption that the intrinsic photopeak efficiency of the detector can be expressed as an exponential function [CA10].

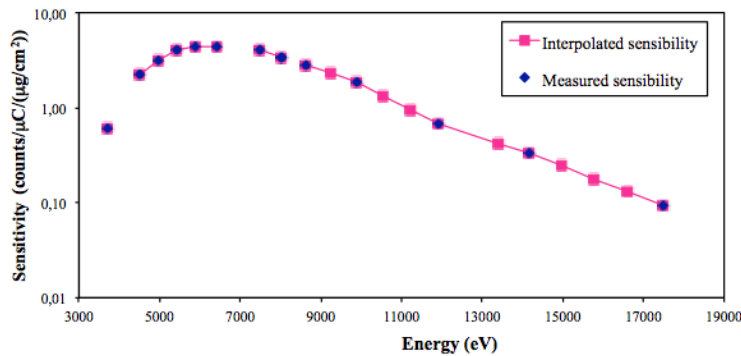


Figure 2.6. Measured and interpolated sensitivity curves for an X-ray detector.

As a quality assurance check of the measured elemental concentrations, a standard reference material, such as the NIST SRM 2783 “Air Particulate on Filter Media” should be always analysed together with the samples. Whereas it is enough measure the MicroMatter standards to obtain the sensitivity curve once per measurement run, it is suggested to repeat the analysis of the NIST SRM 2783 every day of measurement to control and to compensate possible systematic deviations of the experimental parameters (such as detector geometry, beam charge integration...). The certified elemental areal concentrations for the NIST SRM 2783 standard, together with the quoted uncertainties, are shown in Table 2.3, whereas the PIXE spectra of the NIST standard collected with

two SDD devices are shown in Figure 2.7 (see the caption for the experimental details related to the spectra).

Table 2.3. Certified elemental areal concentrations for the NIST SRM 2783 “Air Particulate on Filter Media” standard. For the elements marked with the asterisk () the concentrations are reference values only.*

Element	Areal concentration ($\mu\text{g}/\text{cm}^2$)	Uncertainty ($\mu\text{g}/\text{cm}^2$)
Na	0.19	0.01
Mg	0.87	0.05
Al	2.33	0.05
Si (*)	5.9	0.2
S (*)	0.11	0.03
K	0.53	0.05
Ca	1.3	0.2
Sc (*)	0.00036	0.00003
Ti	0.15	0.02
V	0.0049	0.0006
Cr	0.014	0.003
Mn	0.032	0.001
Fe	2.7	0.2
Co	0.0008	0.0001
Ni	0.007	0.001
Cu	0.041	0.004
Zn	0.18	0.01
As	0.0012	0.0001
Rb (*)	0.0024	0.0006
Sb	0.0072	0.0003
Ba	0.034	0.005
Pb	0.032	0.005

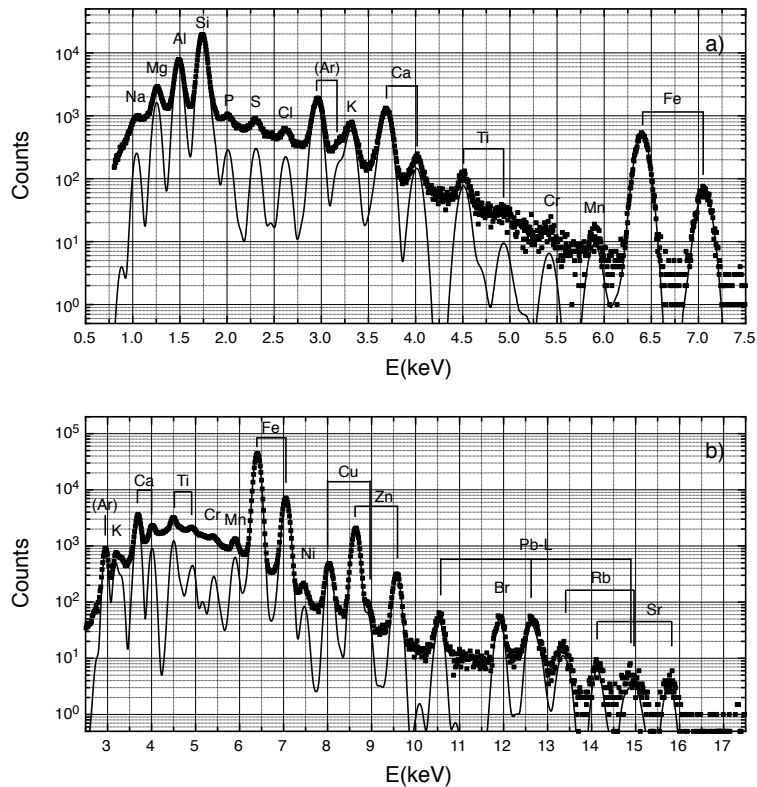


Figure 2.7. PIXE spectra of the NIST SRM 2783 “Air Particulate on Filter Media” standard: panel a) low-Z elements; panel b) high-Z elements), The measurement were carried out in an external beam set-up with proton energy (on target) 3 MeV, beam current 14 nA and measurement time 300 s. The X-ray spectrum of the low-Z elements was collected by a SDD, 30 mm² active area, 8 μm Be window, with helium flowing in front of the detector to minimize air absorption, 8 msr subtended solid angle and 135 eV FWHM energy resolution. The X-ray spectrum of the high-Z elements was collected by a SDD 80 mm² active area, 25 μm Be window, with an additional 450 μm Mylar absorber, 180 msr subtended solid angle and 145 eV FWHM energy resolution.

As an example, Table 2.4 reports the information contained in the GUPIX standard output file corresponding to the analysis of the PIXE spectrum of the NIST SRM 2783 standard shown in panel a) of Figure 2.7. General information and user supplied data relevant for peak fitting and background subtraction are shown together with the resulting element peak areas, uncertainties and the areas used to calculate the limit of detection (see Section 2.2.2).

In case of an homogeneous sample (as produced by LV or HV samplers), a measurement over any part of it gives directly the elemental areal density, according to the above formula; then the total mass of the element Z can be easily obtained by multiplying $(\rho t)_Z$ by the deposit area S .

In case of an inhomogeneous sample (as produced by cascade impactors), the beam has to be scanned over or cover an area larger than the deposit area, then the total mass of the element Z can be obtained by multiplying $(\rho t)_Z$ by the beam spot area A or by the scanned area.

Table 2.4. Contents of the GUPIX standard output for the analysis of the PIXE spectrum of the NIST SRM 2783 standard shown in panel a) of Figure 2.7. Some lines were omitted for the sake of clarity.

```

*** GUPIX (GUelph PIXe): Thin Target Trace Calc ***
      Windows GUPIX2010          Last Update: 2011-02-15
Time: 00:42:41          *** Results ***          Date (y-m-d): 15-02-17

File:IAEAS105.lab          ID:
Chi**2= 11.08      ( 11.08      ) Total counts: 899316 %RMS sys err= 12.33
Total # of loops: 4          Total fit time: 0.0 seconds.
Fit region has 1376 chan ( 125 to 1500). File has 2048 channels.
The detector resolution at the 5.9 keV line is 135.8 eV (150.)
Thin PIXE spectrum acquired(0-12-1714 @ 0:00:00) for 568s.
Trace Average count rate(cps): 1583.3 Average current(nA): 1.761
H: 1.000E+00          Angle(Beam-Target normal) Alpha= 0
Charge: 1.000E+00          (Detector- " " ) Theta= 45
Proton energy(keV): 3040
Looking for 15 elmts: Na K , Mg K , Al K , Si K , P K , S K , Cl K , Ar K ,
K K , Ca K , Ti K , V K , Cr K , Mn K , Fe K
Filters (Z,um,hole fraction):None          Fractional absorber error:0.010
(
Detector efficiency correction of relative intensities: On
Det # 1          SDD Ketek (aerosol) coll
Windows #,(Z,th(cm),g/cm3):1 ( 4,8.00E-04,0.00E+00)
Electrode(Z,cm,hf): ( 13,1.00E-05,0.00E+00) Crystal(Z,cm): (14,4.50E-02)
Sam-Det(cm): 0.00 Ag/At: 1.840 Res(eV):150. Tau(ns): 500. Deadtime(us): 5.0
Use reference proton induced x-ray cross-sections for K & L x-rays.

Peak and spectrum description:
Peak centroid = A1+A2*E+A3*E**2          A(1,2,3): -19.097 179.256 0.0000
Peak width = SQRT(A4+A5*E)          A(4,5): 18.9045 14.9383
With these values the fit region extends from 0.80 to 8.47 keV with FWHM
at center being 123.3 eV or 22.11 channels. Excluding pile-up & escape the
elements have peaks ranging from 0.978 to 7.110 keV.

Background handled by Variable Digital Filter n=fwhm* 1.00 m=fwhm/2* 1.00
Basic peak shape: Gaussian below & Voigtian above peak heights = 1000
Peak plateau: None.
Short step: Energy dependent parameterized short step in use.
Peak tailing: 1 energy dependent parameterized tails per peak.
Matrix abs. edges: None.
Si escape energy in keV: 1.740
Minimum background value for LOD calc: 1
Statistical + Benjamin absorber error channel weighting used (0.010)
Pile-up [99(PU S )] peaks - #allowed: 20, #used: 11

Stopping criteria: STEP:0.0010 LOOPS: 30
Total # of pars., fixed pars. & their IDs: (21, 1) 3

```

#	Elmt	Lay	DF	Peak	2-FWHM	% Fit	% Stat.	+1% Of	LOD	
	Z	Sym.	n/m	Area	Area	Error	Error	Overlap	Area	
1:	11	NaK	/ 0	15/ 8	2493.	3704.	5.92	5.82	5.83	310.7
2:	12	MgK	/ 0	15/ 8	1.6522E+04	2.4466E+04	1.53	1.30	1.32	417.5
3:	13	AlK	/ 0	17/ 8	7.0707E+04	1.0542E+05	0.68	0.41	0.42	409.4
4:	14	SiK	/ 0	17/ 8	2.0825E+05	3.1208E+05	0.49	0.20	0.20	303.6
5:	15	P K	/ 0	17/ 9	3268.	4908.	5.43	4.83	4.93	346.0
6:	16	S K	/ 0	17/ 9	3650.	5450.	4.43	3.93	3.94	305.1
7:	17	ClK	/ 0	19/ 9	2734.	4067.	4.97	4.46	4.51	262.4
8:	18	ArK	/ 0	19/10	2.0967E+04	3.1043E+04	1.03	0.77	0.77	170.9
9:	19	K K	/ 0	19/10	8011.	1.1887E+04	1.87	1.44	1.56	194.6
10:	20	CaK	/ 0	21/10	1.6671E+04	2.4736E+04	1.01	0.77	0.81	153.3
11:	22	TiK	/ 0	21/11	1182.	1755.	5.02	4.14	4.16	78.7
12:	23	V K	/ 0	23/11	0.0000	0.0000	0.00	0.00	0.00	80.9
13:	24	CrK	/ 0	23/12	80.82	119.9	30.51	27.30	27.68	44.1
14:	25	MnK	/ 0	25/12	146.7	217.7	14.38	11.71	11.82	22.9
15:	26	FeK	/ 0	25/12	8897.	1.3376E+04	1.09	0.92	0.92	34.3

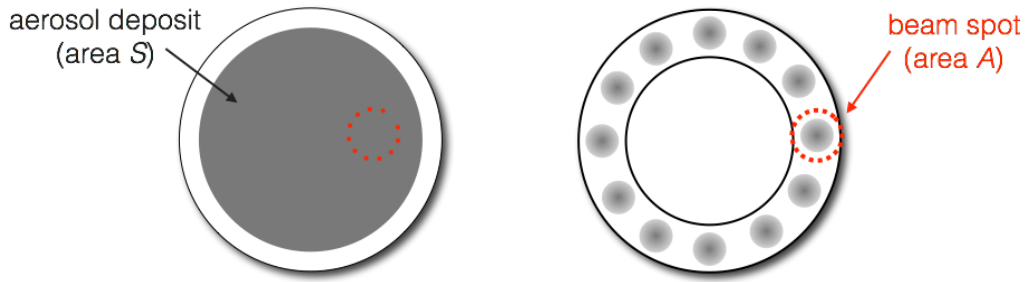


Figure 2.8. Scheme for the measurement of the elemental mass for homogeneous (left picture) and inhomogeneous (right picture) samples. The samples produced by an ISAP1050e sampler are taken as an example.

Then the concentration in air, i.e. in ng/m^3 , of the element Z can be obtained dividing the element mass by the sampled volume, V

$$(\rho t)_Z [\text{ng/m}^3] = 1000 \cdot (\rho t)_Z [\mu\text{g/cm}^2] \cdot S [\text{cm}^2] / V [\text{m}^3] \quad (2.4)$$

where S is the deposit area in case of homogeneous sample or it is the scanned beam area in case of an inhomogeneous sample. Considering the example made before on the Na concentration in the PM2.5 aerosol sample, assuming a 47 mm diameter filter (typically 11.9 cm^2 deposit area) and a sampling for 24 hours at $2.3 \text{ m}^3/\text{h}$ (sampled volume 55.2 m^3), the Na concentration in air, expressed in ng/m^3 , would be $1000 \cdot 1.74 \mu\text{g/cm}^2 \cdot 11.9 \text{ cm}^2 / 55.2 \text{ m}^3$, corresponding to $(\rho t)_{\text{Na}} = 375 \text{ ng/m}^3$.

2.2.2 Detection limits

Generally, an X-ray peak is considered detectable if its intensity exceeds a three-standard-deviation fluctuation of the underlying background (Minimum Detection Limit, MDL), which may comprise contributions from Bremsstrahlung, nuclear reaction gamma-rays and overlapping X-rays. The continuous background in PIXE spectra is mainly due to secondary electron Bremsstrahlung radiation (from the filter more than from the aerosol sample) for energies typically below 10 keV. The endpoint energy T_m of the SEB radiation spectrum is given by $T_m = 4m_e E_0 / m_p$, where m_e and m_p are the electron and proton mass respectively and E_0 is the proton beam energy. For example, for 3 MeV protons, the endpoint energy of the SEB radiation spectrum is about 6 keV. The intensity of the SEB radiation spectrum increases with the proton beam energy, as shown in Figure 2.9.

A contribution from Compton interaction in the X-ray detector active volume from gamma-rays emitted typically by the filter (e.g. F from Teflon) more than by the aerosol sample, is possible in the energy region above 10 keV, as shown in Figure 2.10.

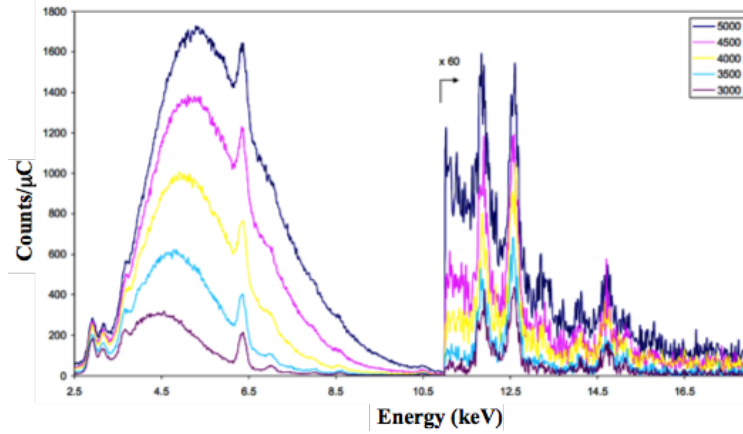


Figure 2.9. PIXE spectra of a PM10 aerosol sample collected on Nuclepore with a Si(Li) detector (with a 450 μm Mylar absorber) for different proton beam energies (listed in keV in the legend). Proton beam current was 15 nA and measurement time 400 s.

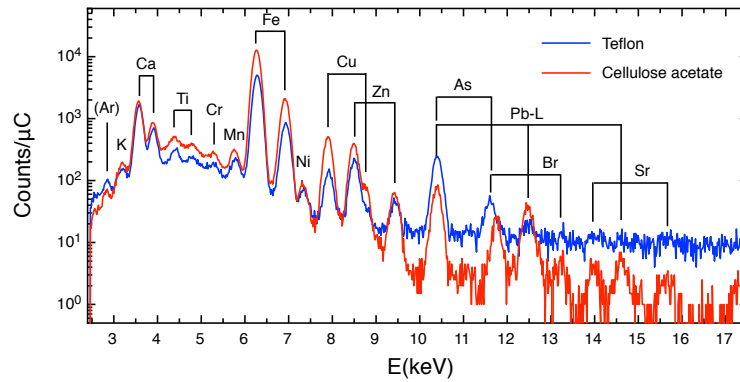


Figure 2.10. Normalized PIXE spectra of a PM10 aerosol sample collected on Teflon (blue line) and on a Cellulose Acetate (red line) filters. Proton beam energy 2.85 MeV, beam intensity 5 nA. The increased background in the spectrum region above 10 keV for the measurement on Teflon filter is clearly evident.

In terms of areal density (i.e. $\mu\text{g}/\text{cm}^2$) the MDL can be calculated as:

$$MDL_z = \frac{3 \cdot \sqrt{N_B}}{\eta_z \cdot Q} \quad (2.5)$$

where N_B is the number of counts integrated in a region of the background under the peak as wide as the peak FWHM, η_z is the corresponding sensitivity value for the specific element and Q is the beam charge during the measurement. It has to be noted that using GUPIXWin for PIXE spectrum fitting, $3 \cdot \sqrt{N_B}$, the numerator of Formula 2.5, is equal to the “LOD area” value calculated by GUPIX (see Table 2.4).

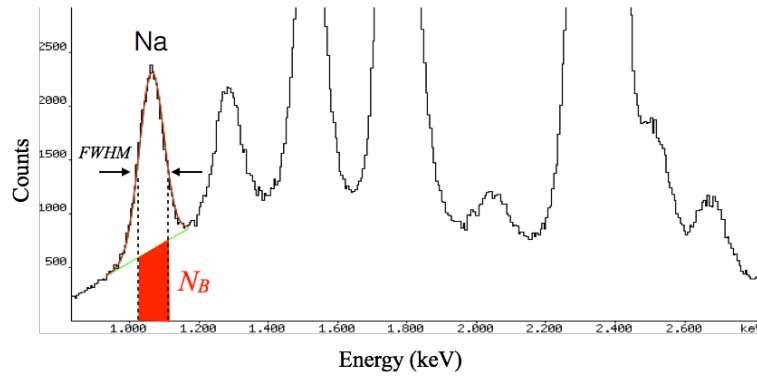


Figure 2.11. Example of the procedure for determining the background area for the calculation of MDL for a sample element (Na in the shown case). The PIXE spectrum is the same shown in panel a) of Figure 2.4.

For example, the MDL for Na in the PM2.5 aerosol sample shown in Figure 2.11, can be calculated as follows. The number of counts integrated in the FWHM-wide region of the background under the Na peak, N_B , resulted around 11200 counts. Considering that the aerosol sample was analysed with an integrated charge, Q , of 5.37 μC and that the sensitivity value for Na was $\eta_{Na} = 2995 \text{ counts}/\mu\text{C}/(\mu\text{g}/\text{cm}^2)$, the obtained detection limit for Na was $\text{MDL}_{Na} = 3 \cdot (11200)^{1/2} / (2995 \cdot 5.37) = 0.02 \mu\text{g}/\text{cm}^2$.

A comparison between PIXE and XRF detection limits that can be obtained with typical instrumentation and experimental conditions is shown in Figure 2.12. PIXE analyses were carried out with a 3.0 MeV proton beam, using SDD and Si(Li) detectors for elements lighter and heavier than above Ca respectively, and beam currents of 6 nA (Teflon) and 12 nA (Polycarbonate), for 10 minutes. XRF analyses were carried out using a commercial Oxford ED-2000 spectrometer equipped with a 50 W Ag anode tube and a Si(Li) detector. Measurement conditions were: 15 kV anode voltage, 0.1 mA anode current for 1000 s for the analysis of elements from Na to P; 30 kV anode voltage, 0.5 mA anode current, a 50 μm thick Ag primary filter for 3000 s for the analysis of elements from S to Pb, for a total measurement time of 1 hour per filter.

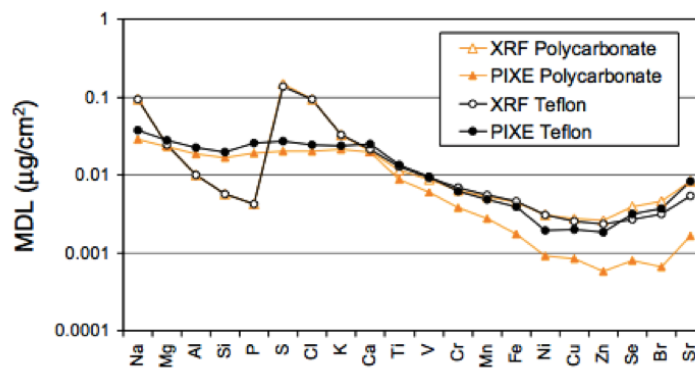


Figure 2.12. PIXE and XRF MDLs, for different elements, for APM samples collected on polycarbonate and Teflon filters. Reproduced from [CA08].

The choice of the proton beam energy for PIXE is always a compromise between the need to increase the energy to increase the X-ray emission cross section of the mid- high-Z elements (enhancing their detection limits) and the need to decrease the energy to reduce the extent and the intensity of background due to the secondary electron Bremsstrahlung. In the analysis of atmospheric aerosol samples, since they are thin targets, there is no need to increase the proton beam energy to increase the probed depth into the sample.

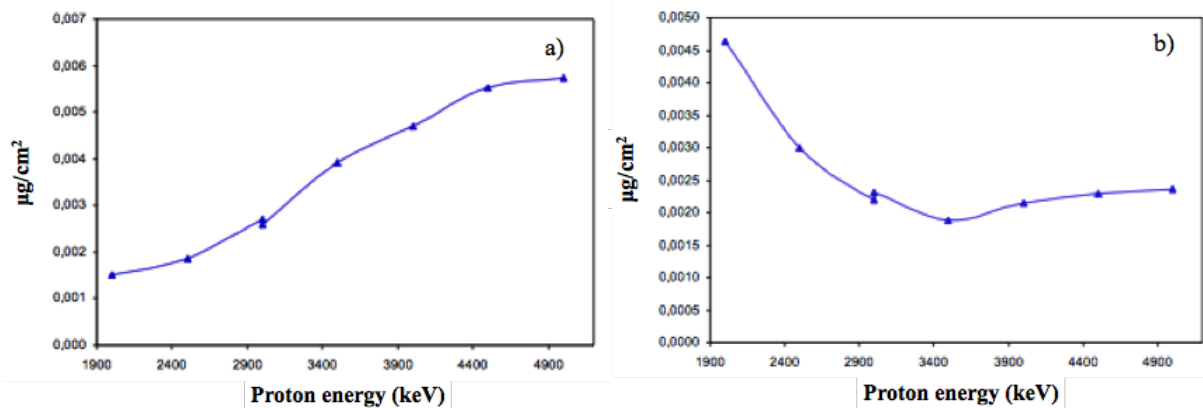


Figure 2.13. Minimum detection limits for: a) Mn and b) Sr in aerosol samples collected on Nuclepore filters as a function of the bombarding proton beam energy.

Note that in the case of analysis of aerosols collected on Teflon (CF_2) filter the choice of the proton beam energy is actually dictated by the need of limiting the gamma-ray emission from Fluorine in the filter, i.e. avoiding strong resonances in the $^{19}\text{F}(p,p'\gamma)^{19}\text{F}$ inelastic reactions producing 110 and 197 keV gamma-rays, that will increase the continuous background in the PIXE spectra in the energy region >10 keV, increase pile-up and dead-time effects and eventually paralyze the X-ray detector (obviously the thicker the detector, the more critical are these effects).

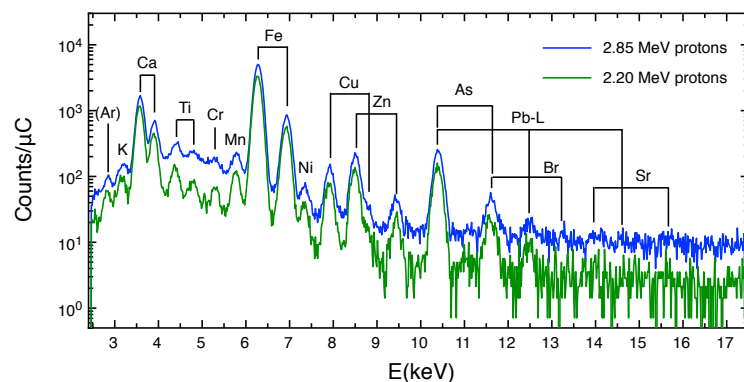


Figure 2.14. PIXE spectra of a APM sample collected on Teflon filter measured at two proton beam energies. The increase in the continuous background in the X-ray energy region >10 keV for the measurement at 2.85 MeV proton is evident.

On the basis of finding bombarding energies that lead to relatively minimal values of the cross section for the $^{19}\text{F}(p,p\gamma_{1-0})^{19}\text{F}$ (gamma-ray energy 110 keV) and $^{19}\text{F}(p,p\gamma_{2-0})^{19}\text{F}$ (gamma-ray energy 197 keV) inelastic reactions, the suggested proton beam energies (energy on target) are, for example, 3.0, 2.5, 2.2 and 1.6 MeV.

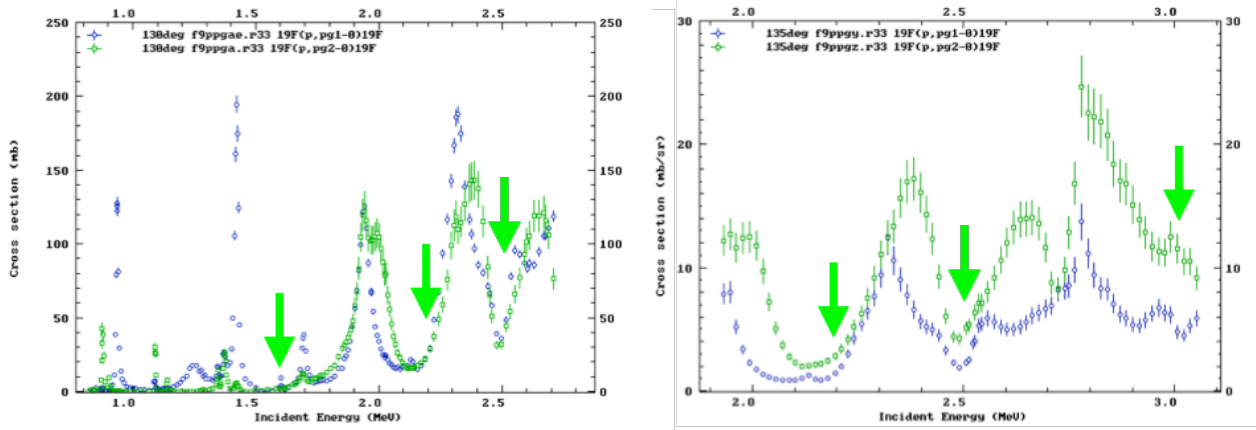


Figure 2.15. Cross section for the production of 110 keV (blue points) and 197 keV (green points) gamma-rays from $^{19}\text{F}(p,p'\gamma)^{19}\text{F}$ reactions, as a function of proton energy from [JE00], left plot, and [ZA15], right plot. The arrows marks minima in the cross section at the energy of 1.6, 2.2, 2.5 and 3.0 MeV.

Beside the choice of a proper proton beam energy, as discussed above, to improve the MDLs in the analysis of APM samples collected on Teflon filters, the use of SDD instead of Si(Li), having detector thicknesses one order of magnitude less (0.5 mm for SDD as compared to 3-5 mm for Si(Li), see Table 2.2), will result in a remarkable reduction of the gamma-ray Compton background without affecting the detector efficiency in the 10-20 keV range.

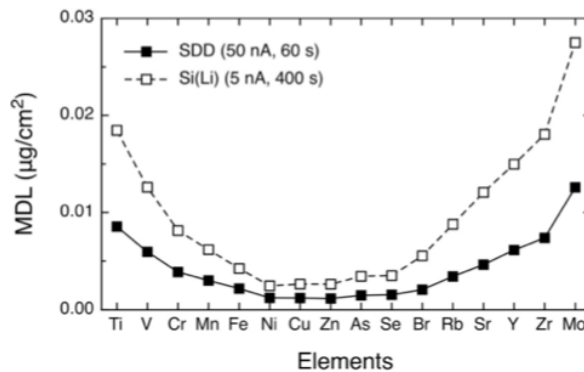


Figure 2.16. Comparison between the MDLs for the various elements detectable with the Si(Li) and with the SDD in a 3.0 MeV proton PIXE measurement on a Teflon filter. For the Si(Li) the measurement lasted 400 s at a beam current 5 nA, while for the SDD lasted only 60 s at a beam current of 50 nA, in order to keep the integrated dose very similar. Reproduced from [LU14].

2.2.3 Uncertainty budget

The experimental uncertainties on the elemental concentrations (ng/m^3) measured by PIXE are given by the sum of independent uncertainties on the flux measurement (about 2-3%), on certified standard elemental concentrations (5%), on beam charge measurement (about 1%) and on peak areas. The uncertainty on peak areas includes the X-rays counting statistics and all the fitting uncertainties (background subtraction, peak overlaps, etc.). The counting statistics uncertainty may vary from few percent up to 20-30% or more when concentrations approach minimum detection limits (MDLs). It has to be noted that the uncertainty on the certified standard elemental concentration is systematic for all the same elements (different samples), whereas the uncertainty on the beam charge measurements is systematic for all the concentrations from the same sample (different elements).

5. Feasibility of IBA measurements of APM samples with ambient pressure set-ups

IBA techniques are easily performable with an external beam, i.e. with ion beam extracted from the vacuum beam line of the accelerator into ambient pressure through a thin extraction window typically glued to the end part of the vacuum beam line (exit nozzle). The sample is then placed typically at about 1 cm distance from the window.

The advantages in working with an external beam set-up can be summarized as:

- direct analysis of filters having any size and shape;
- no sampling;
- no charging effects, no need of sample pretreatment (i.e. conductive coating);
- no heating, thus drastically reducing the risk of selective loss of some more volatile aerosol components (like Cl, Br and ammonium) under beam irradiation during in-vacuum measurements;
- easy sample positioning;
- fast and efficient.

The limitations in working with an external beam set-up are:

- actual restriction to the use of protons (to reduce the increased energy straggling of heavier ions in passing through the exit window and the path in atmosphere);
- need of an He flow in front of the X-ray detector to avoid attenuation of the low-energies X-rays in normal atmosphere (1 cm of air absorbs completely 1 keV X-rays, while in 1 cm of He the transmission is 99%);
- beam energy loss;
- beam energy straggling;
- increased beam lateral spread.

Some of these limitations are thus making external beam EBS analysis less attractive than in a in-vacuum set-up.

The window material and its thickness have to be chosen in order to guarantee:

- resistance to the pressure gradient;
- resistance under beam irradiation;
- to be thin enough not to affect too much the beam properties (energy and angular resolution);
- to produce no or negligible background radiation when traversed by the beam.

Typical choices for these applications are 7.5-8 μm thick polymeric films (Kapton, $\text{C}_{22}\text{H}_{10}\text{N}_2\text{O}_5$ or Upilex, $\text{C}_{22}\text{H}_{10}\text{N}_2\text{O}_4$) or 100-500 nm thick inorganic membranes (Si_3N_4). The effect on 3 MeV protons passing through these two type of extraction windows and then traversing 1 cm of He before impinging on the sample are indicated in the following table.

Table 5.1. Energy loss and energy straggling of 3 MeV protons through typical extraction windows for ambient-pressure IBA analysis of APM samples.

Window type	Energy loss	Energy straggling, FWHM
8 μm Kapton/Upilex	145 keV	20 keV
500 nm Si_3N_4	40 keV	12 keV

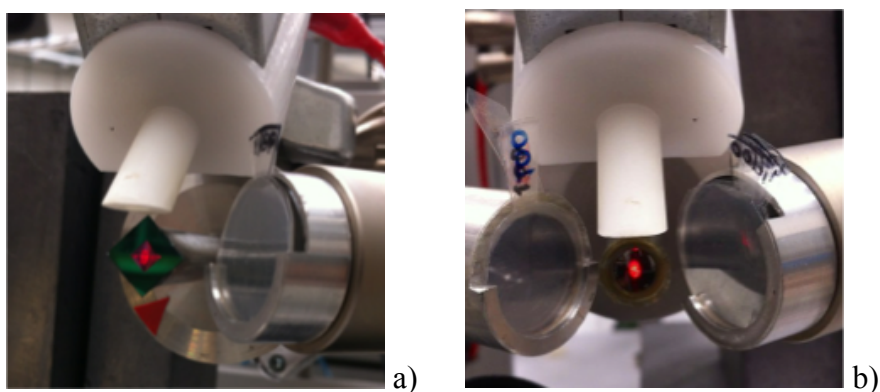


Figure 5.1. Pictures of exit nozzles for external beam PIXE set-ups with 500 nm Si_3N_4 (a) and 8 μm Upilex (b) extraction windows.

The installation of a dedicated external beam set-up for IBA analysis of aerosol samples is actually more cost effective than installing a dedicated in-vacuum set-up, since the initial costs for purchasing a scattering chamber and a high-vacuum system are not present. Anyhow, it has to be stressed that for good IBA measurements in an external beam set-up the use of He gas flow is mandatory to reduce both the beam energy loss and straggling in the path in atmosphere and the absorption of the low-energy X-rays, so a supply of He gas canisters has to be guaranteed.

Since it is useful to analyse the largest area as possible of the sample in order to average out possible sampling/collection inhomogeneties, the IBA practitioner is faced with two possibilities: using a broad beam (typically 8-10 mm diameter) or a more collimated/focused beam (beam spot about a few mm^2) and then mechanically scanning the sample. The feasibility of these two options with respect to in-vacuum or external-beam set-ups is indicated in the following table.

Table 5.2. Feasibility of IBA analysis of APM samples with broad or collimated beams in external beam or in-vacuum set-ups.

Set-up	Broad beam	Collimated beam w/scanning
In-vacuum	X	X
External beam		X

In this regard sample scanning is much more technically feasible and cost effective with an external beam set-up, since there is no need of vacuum actuators.

Note that using the broad beam option makes the definition of the subtended solid angle of the detectors less reliable and if a collimated detector is used some care has to be taken to ascertain that the field of view of the collimated detector cover the whole broadly irradiated area. Moreover the broad beam is not indicated in case Elastic Scattering techniques are intended to be used.

6. Bibliography and references

M. Nastasi, J.W. Mayer, Y. Wang “*Ion Beam Analysis - Fundamentals and Applications*”, CRC Press, 2014

Y. Wang, M. Nastasi ed.s “*Handbook of Modern Ion Beam Materials Analysis*”, 2nd ed., MRS Publishing, 2009

B. Schmidt, K. Wetzig “*Ion Beams in Materials Processing and Analysis*”, Springer, 2013

S. A.E. Johansson, J.L. Campbell, K.G. Malmqvist ed.s “*Particle-induced X-ray emission spectrometry (PIXE)*”, John Wiley & sons, 1995

W.-K. Chu, J.W. Mayer, M.-A. Nicolet “*Backscattering Spectrometry*”, Academic Press, 1978

[CA06] G. Calzolari et al., Nucl. Instr. and Meth. B 249 (2006) 928

[CA08] G. Calzolari et al., Nucl. Instr. and Meth. B 266 (2008) 2401

[CA10] J.L. Campbell et al., Nucl. Instr. and Meth. B 268 (2010) 3356

[CA15] G. Calzolari et al., Nucl. Instr. and Meth. B 363 (2015) 99

[FE02] M. Fedi et al., Nucl. Instr. and Meth. B 189 (2002) 56

[GA84] E. Gatti and P. Rehak, Nucl. Instr. and Meth. 225 (1984) 608

[IA03] IAEA TECDOC No. 1342, “Intercomparison of PIXE spectrometry software packages” (2003)

[JE00] A.P. Jesus et al., Nucl. Instr. and Meth. B 161-163 (2000) 186

[JE12] C. Jeynes et al., Nucl. Instr. and Meth. B 271 (2012)

[JO70] T.B. Johansson et al., Nucl. Instr. and Meth. 84 (1970) 141

[LU11] F. Lucarelli et al., X-Ray Spectr. 40 (2011) 162

[LU14] F. Lucarelli et al., Nucl. Instr. and Meth. B 318 (2014) 55

[MA15] W. Maenhaut, Nucl. Instr. and Meth. B 363 (2015) 86

[RU57] S. Rubin et al., Anal. Chem. 29 (1957) 736

[ZA15] I. Zamboni et al., Nucl. Instr. and Meth. B 342 (2015) 266

Appendix A

The following table lists the various categories of filters (fibre filters and membrane filters) and the different nuclear analytical techniques (ED-XRF, PIXE, PIGE, Elastic Scattering Techniques, i.e. EBS and PESA) that can be positively used and what information can be obtained.

Filter	ED-XRF	PIXE	PIGE	EBS	PESA
Glass	X ^a	X ^b	X		
Quartz	X ^a	X ^b	X		
Cellulose	X	X	X		
Nuclepore	X	X	X		
Teflon	X	X ^c		X	X

^a Only from S on; strong attenuation from the filter material is expected for low-Z elements (up to Ca) due to penetration of particles in the fibre filters

^b From Na on (obviously not Si) if SDD is used, otherwise typically from S on; strong attenuation from the filter material is expected for low-Z elements (Na-Ca) due to penetration of particles in the fibre filters

^c Mid- high-Z elements can be analysed with good MDLs only if specific proton beam energies are selected

Appendix B

The following table lists typical detection limits and experimental uncertainties for IBA analysis of APM samples, referring to 5-6 minutes of measurements with 3 MeV protons and 5-10 nA proton beam intensity

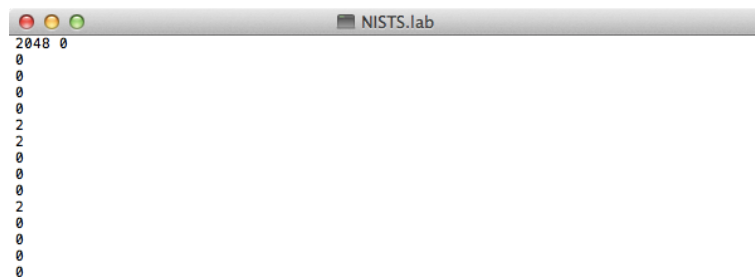
Element	IBA technique	Typical detection limit ($\mu\text{g}/\text{cm}^2$)	Typical detection limit (ng/m^3) ^a	Total uncertainty
H	PESA	0.1	20	5-10%
Li	PIGE	0.04	8	5-20%
B	PIGE	0.04	8	5-20%
C	EBS	4.0	800	5-10%
N	EBS	2.0	400	10-30%
O	EBS	2.0	400	10-20%
F	PIGE	0.05	10	5-20%
Na	PIGE	0.04	8	5-20%
Al	PIGE	0.07	15	5-20%
Na-V	PIXE	0.05	10	5-20%
Cr-Pb	PIXE	0.01	2	5-20%

^a Considering a 47 mm diameter filter and sampling for 24 hours at 2.3 m³/h (European standard, EN12341)

Appendix C

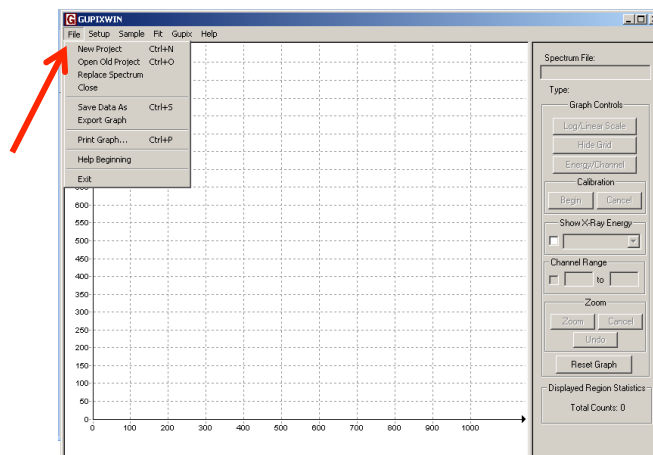
In the following some hints and instructions on how to apply the GUPIXWIN, the Guelph PIXE software package, to the analysis of PIXE spectra of APM samples will be provided. GUPIXWIN is here proposed to be used to obtain X-ray peak areas and then quantitative analysis is obtained by comparison with standards, so these instructions should not be directly transferred to other cases. Please refer to GUPIXWIN instruction manual for basic information on the software capabilities and working principles or for further details, for example for modifying and inserting custom data in the AP0DET.DAT detector file.

- 1) It is suggested to create a new folder containing the spectrum files. This same folder will be used to save all the GUPIX output files. The format of the spectrum file (extension .LAB) is, for instance, the following:



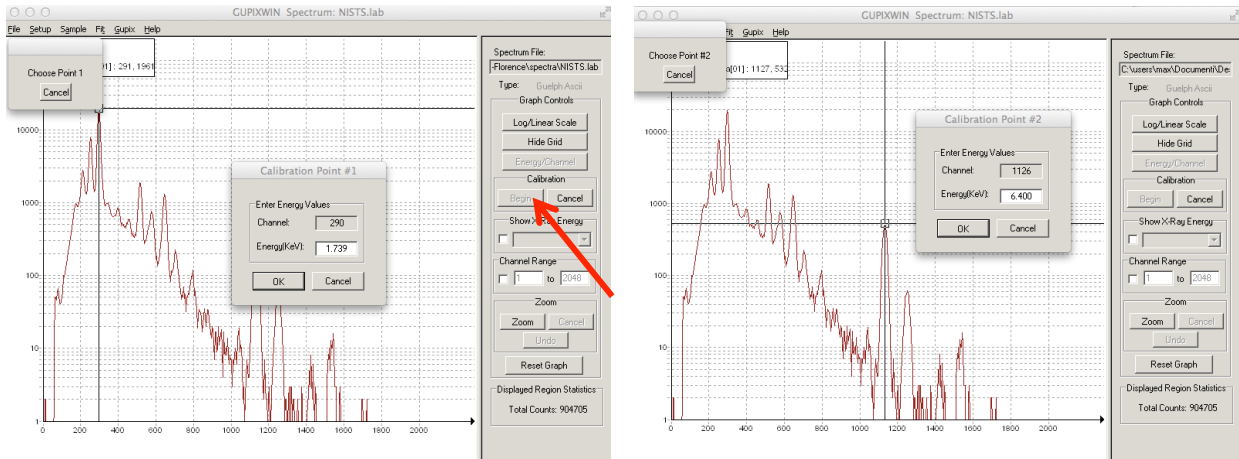
i.e. a first line containing two values, the first one stating the number of channels in the spectrum (2048 in the example shown) and the second one that can be either 0 or 1. If it is 0, as in the example, then the first line is followed by a single column of the counts per channel; please note that the maximum number of allowed channels is 2048.

- 2) If no other previous analysis project file (extension .PAR) already exists, a new one has to be created (*File/New project*) and the user is prompted to open a spectrum file (see above).



In case it were possible to start from a previous analysis file (*File/Open old project*), then the old spectrum has to be replaced with one of the new ones (*File/Replace spectrum*).

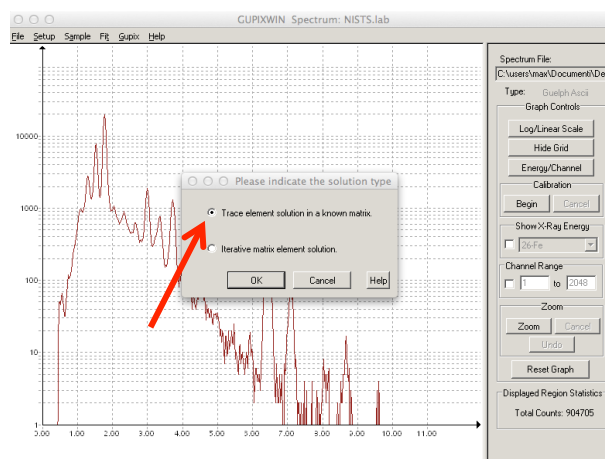
3) Spectrum calibration



After pressing the button *Begin* the user is prompted to select with the cursor a first peak (among two). In the example, referring to PIXE spectrum of the NIST SRM 2783 standard (see panel a) of Figure 2.7), the first peak is the Si $K\alpha$ line, and its X-ray energy (1.739 keV) has to be written in the empty field *Energy(keV)*. After pressing *Ok*, then the user is prompted to select a second peak. In the example the second peak is the Fe $K\alpha$ line, with X-ray energy 6.400 keV. At the end press *OK*. Afterwards, to check the accuracy of the energy calibration tick the *Show X-Ray energy* option and visually check the peaks-to-element correspondence by selecting different elements in the drop-down menu.

4) Routine selection

In the *Setup* menu select the *Trace or Matrix* command. Then in the new pop-up window check the solution type *Trace element solution in a known matrix*. Press *OK*.

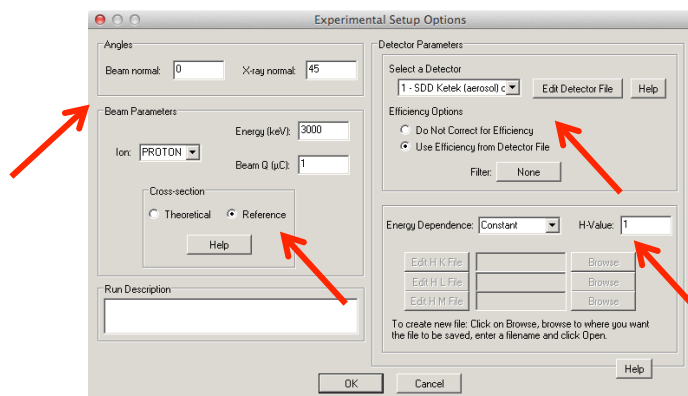


5) Experimental set-up

Now in the *Setup* menu select the *Setup* command.

In the *Experimental Setup Options* window the user can insert the relevant experimental details, such as:

- the values of the angle formed by the incoming beam and the sample normal and the angle formed by the X-ray detector and the sample normal (in the example shown, the sample is perpendicular to the beam and the X-ray detector is placed at 45°);
- the ion beam particles (protons);
- the actual beam energy on the target, in keV (in the example shown, 3000);
- for beam charge the user can insert an arbitrary value, for example 1 (it has to be noted that GUPIX is here proposed to be used to obtain only peak areas and then quantitative analysis is obtained by comparison with standards, so some of the requested data can be easily substituted with arbitrary values);
- choose *Reference* cross section;
- choose a *Constant* energy dependence (default value) of the instrumental factor, with H-value equal to 1.

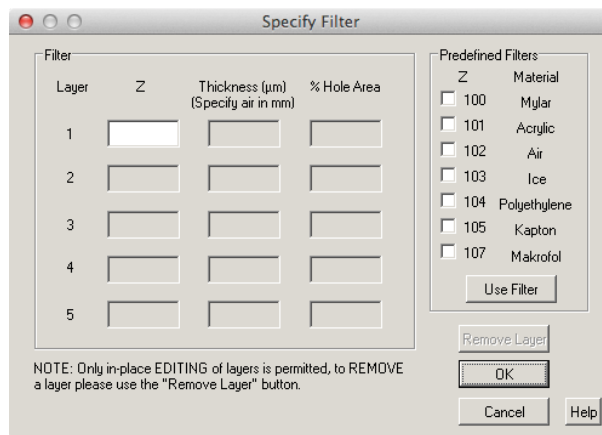


The user has to select the detector from the APODET file; at this step the user can also modify the detector file (by pressing the button *Edit Detector File*). The default APODET file has already generic parameters for typical SDD and a Si(Li) detectors; following the instruction in the GUPIXWIN manual the user can anyway refine some specific parameters, such as thickness and material of the detector entrance window, the crystal thickness, the target-to-crystal distance and the detector energy resolution. For the detector efficiency check the option *Use Efficiency from Detector File*.

In case a filter or filters were present, the user has to define it/them by clicking on the appropriate button (default value is *None*, and it turns into *Active* when a filter is present) and inserting the relevant data in the *Specify Filter* pop-up window.

It is to be noted that “filter” is everything in between the target and the detector, for example: external path (typically He or air), absorber for low energy X-rays, filter with hole (“funny filter”) for one-detector experiments. The user must indicate atomic number and thicknesses of the filters, and tabulated materials can be used. Press *OK* once finished.

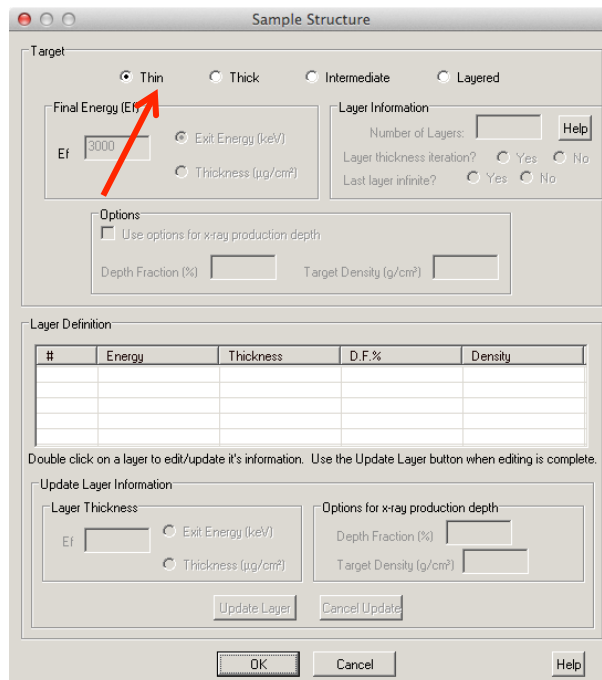
Once all measurement parameters have been inserted press *OK* to close the *Experimental Setup Options* window.



6) Sample

In the *Sample* menu select the *Sample* command.

In the *Sample Structure* window select the *Thin* target option (default value), meaning that matrix effects are neglected, then press *OK*.



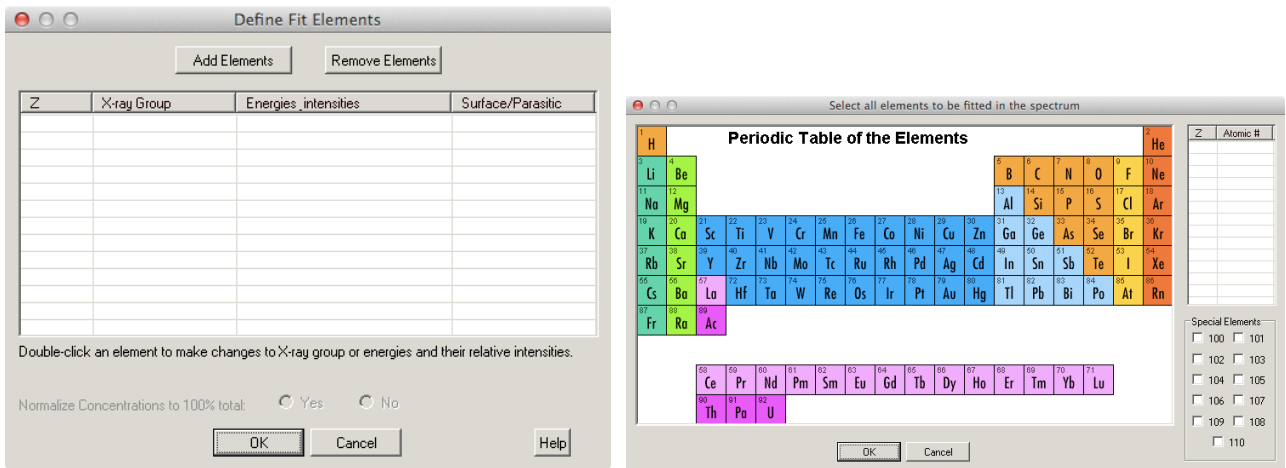
In the *Sample* menu select *Trace Element Solution* and then the *Define Fit Elements* command.

In the *Define Fit Elements* window click on the *Add Elements* button.

A periodic table of the elements will appear in a new pop up window; the user can add all the elements to be fitted in the spectrum by clicking on them (and they will then appear on the list on the right-hand side of the window).

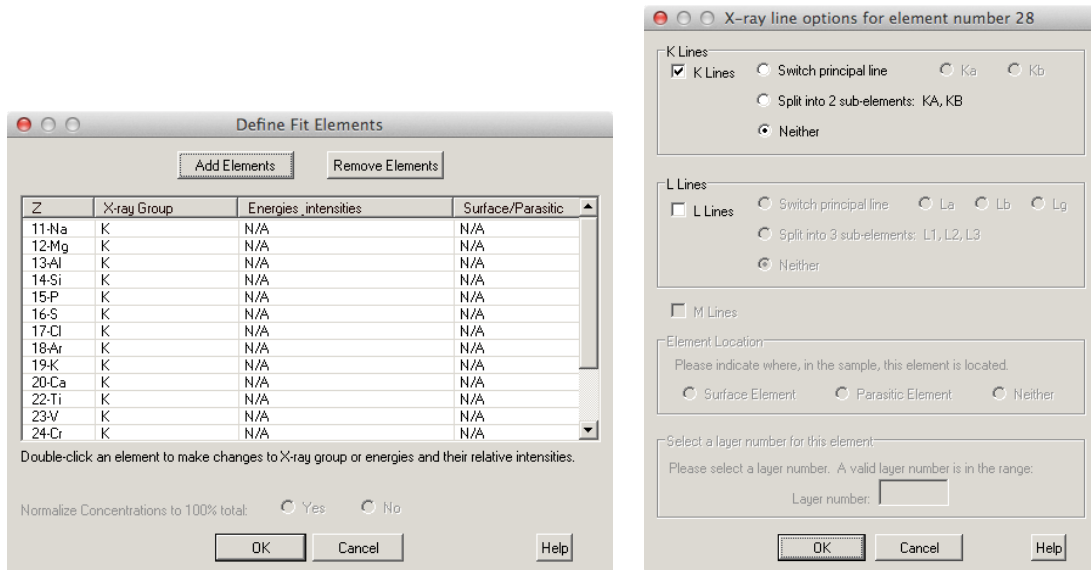
The elements to be considered in a PIXE spectrum of an APM sample are typically:

- from Na to Zr, with the exclusion of Sc, Co, Ga and Ge, for the K-line X-rays. Ar and Kr should be included when the measurements are performed in an external beam set-up, otherwise these two elements can be excluded;
- Pb, Ba for the L-line X-rays.



The range of elements to be included in the fit depends essentially on the detector intrinsic efficiency, i.e. on detector properties such as thickness, entrance window and dead layers, and on composition and thickness of absorber foils eventually are placed in front of the detector.

Once finished inserting all the elements press *OK*.



Back in the *Define Fit Elements* window it is possible to add other elements or remove some. Double clicking on an element the user can then indicate:

- the lines to be fitted (selecting K lines and/or L lines)²;
- whether the element is to be considered *parasitic* (when the related X-rays do not come from the analyzed sample, such as the case of Ar or Kr in external beam PIXE measurements) or as *surface* element (e.g. contained in a contamination layer, but this case is rarely found in the APM sample analysis).

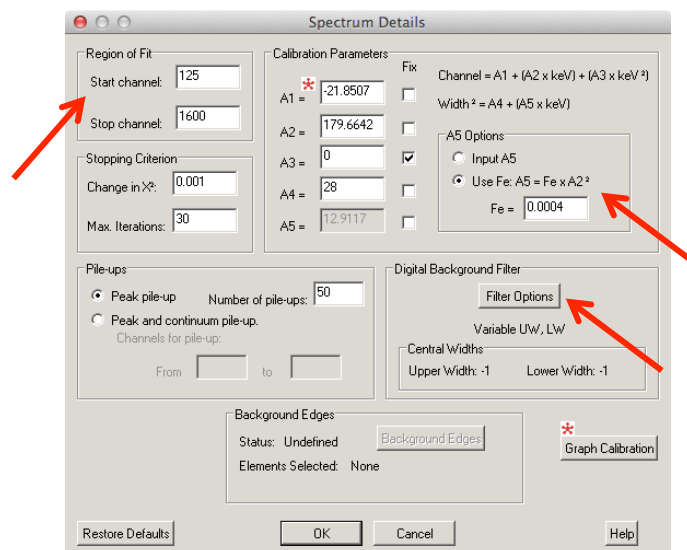
It is to be noted that the possibility of indicating if an invisible element (such as O, for example bound to visible elements to form oxides, a common situation in the analysis of glass samples) is present in the sample as well is neglected in the analysis of APM samples.

Once all the elements have been inserted press *OK* to close the *Define Fit Elements* window.

7) Fit

In the *Fit* menu select the *Spectrum Details* command.

In the *Spectrum Details* window the user can select the fitting parameters. For example:



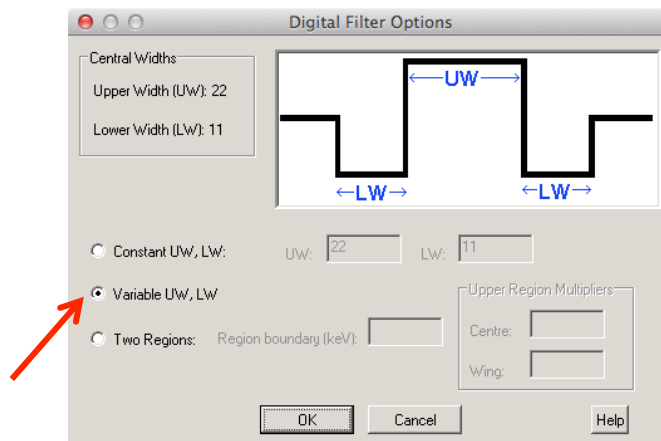
- as region of fit it is convenient to choose appropriate start and stop channels to avoid fitting over irrelevant portions of the spectrum (typically in the low and high energy range of the spectrum);
- the calibration parameters A1 and A2 (channel vs energy offset and slope) are already calculated after the energy calibration of the spectrum. It is possible to introduce a quadratic term in the channel vs energy dependance (A3), but it is suggested to fix it to 0³. The calibration parameters A4 and A5 describe the widening of the peak FWHM with the X-ray energy, e.g. $FWHM(E) = 2.35 \cdot (A4 + A5 \cdot E)^{1/2}$ where A4 is the electronic noise (value

² It is mandatory for Ba since K-lines are selected by default.

³ It has to be noted that for some SDD fixing A3 to 0 might result in a worse fit; the analyst is thus suggested to try different approaches, whether keeping A3 fixed to 0 or keeping it free (unticking the box), then choosing the one yielding the best fit.

around 30 is typical for SDD and Si(Li)), while $A5$ is the energy-dependent resolution factor, depending on the Fano factor ($F = 0.11$ for Silicon) and the average energy to produce a charge carrier in the semiconductor detector ($e = 3.6$ eV for silicon). Checking the second option for the calculation of $A5$ parameter (e.g. *Use Fe: $A5 = Fe \times A2^2$*) the user should insert a value of $Fe = 0.0004$ in the empty field. Please note that if the *Fix* boxes are not ticked (as suggested) then the calibration parameters are allowed to vary during the fit to improve the fitting results;

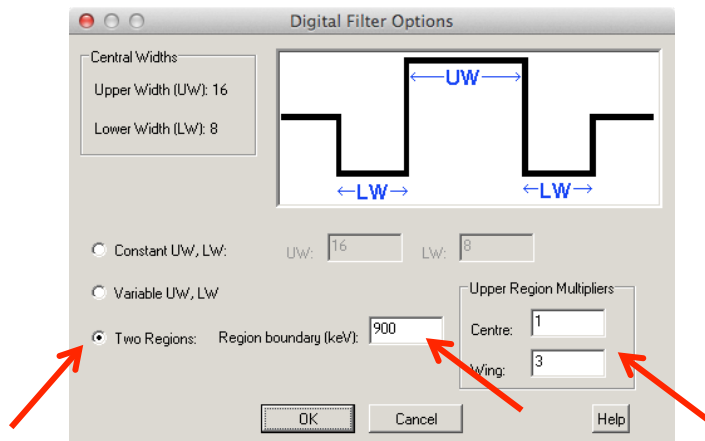
- GUPIX can evaluate pile-up contributions as sum of principal lines events or can evaluate a continuum pile-up from an energy region defined by the user (time consuming, but useful when pile-up effects come from an energy region not included in the spectrum); please use the default values;
- for background subtraction the software applies to the spectrum a top-hat digital filter to remove the components at low frequencies in data spectrum; the choice amongst three filters (constant, variable or two-region variable width filter) is made after clicking on the *Filter Options* button.



It is suggested to use a variable filter (*Variable UW, LW*), since peak widths change significantly passing from the low energy to the high energy side of the spectrum. The variable digital filter indeed allows the filter dimensions to change as the FWHM changes from channel to channel thus allowing this “optimal compromise” filter to be used throughout the fit region.

In some cases (especially in the higher-energy regions of PIXE spectra of APM samples collected on Telfon filters having only a small number of weak peaks and very little overlap, and weak, slowly varying background, due to Compton interaction in the X-ray detector active volume from gamma-rays, see Figure 2.10) the best filter is a two-region variable digital filter, with the two regions separated by a user-defined energy. The separation should define a low energy region where the Bremsstrahlung background hump is evident and significant peak overlap occurs, and a high-energy region of low background intensity. Such *Region boundary*

should be inserted in channels and not in keV, as erroneously written in the command window, and it should correspond roughly to the end of the SEB background.



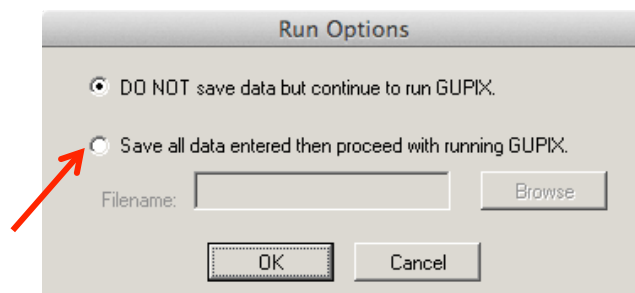
For instance, in the shown example a region boundary at channel 900 corresponds to an energy of 900 divided by the A2 calibration parameter (i.e. channel vs energy slope), that is $900 \text{ channels} / 179.7 \text{ channels} \times \text{keV} = 5 \text{ keV}$ (the endpoint energy of the SEB background is 6 keV for 3 MeV protons, see section 2.2.2). Below the energy cut-off, a variable digital filter is automatically used by GUPIX; above the cut-off the user can specify a wider filter to obtain better-fitted peak areas. It is suggested to use the following values for the *Upper Region Multipliers*: 1 for *Centre* and 3 for *Wing*, as shown in the example. Once finished selecting the *Filter Options* press *OK*.

Then, once finished inserting all the spectrum details for the fitting procedure press *OK*.

8) Gupix

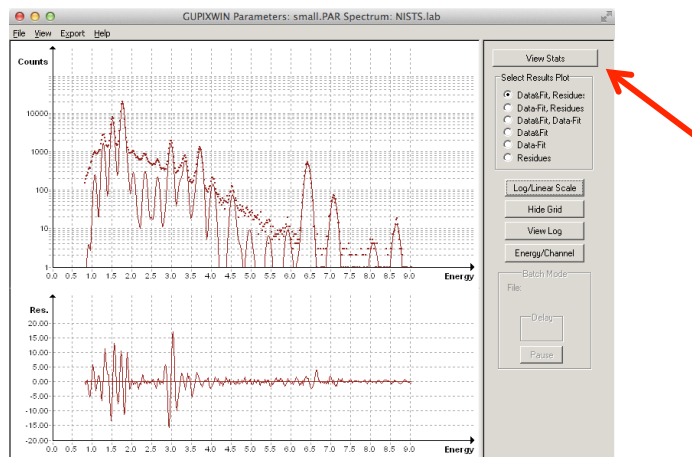
In the *Gupix* menu select the *RUN* command.

In the *Run Options* window the user should save all data entered so far, creating a .PAR file (it is suggested to create it in the same folder containing the spectrum files) then proceed with running GUPIX, pressing *OK*. This .PAR file will be then opened and used for further analysis and for automatic analysis of a large batch of spectra.



Once the fitting procedure has finished and successfully converged (a pop-up window with some warnings could appear), the user should see a window like in the following example. In the

upper panel there is the original spectrum with the fitted X-ray peaks while in the bottom panel residuals (experimental spectrum minus fitted peaks minus subtracted background) are shown. Residuals give an estimate of how good the fit is. Other plotting options are available.

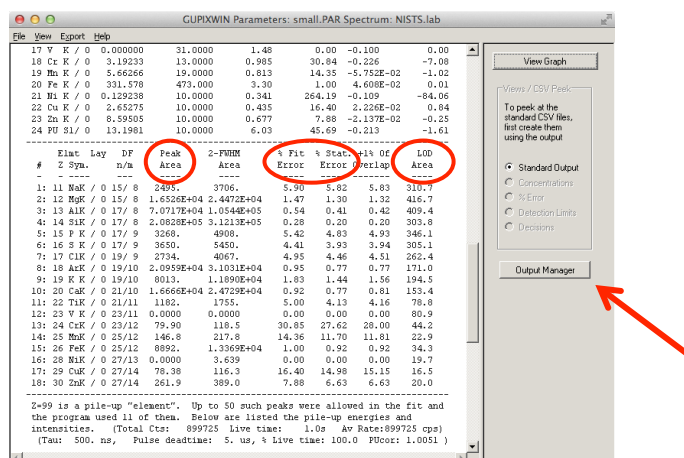


Check that all the peaks have been fitted. Residuals should be symmetrical with respect to zero and not exceeding, as a rule of thumb, 20 (actually this value depends on and has to be compared with the number of counts in the corresponding peak). Large peaks in the residuals may suggest not fitted peaks in the spectrum.

In case the fit is not good it can be possible to improve it by (in order of effectiveness):

- 1) checking the energy calibration;
- 2) checking if some element is missing;
- 3) using a constant or variable A3 parameter in the energy calibration;
- 4) changing the top-hat digital filter.

By clicking on the *View Stats* button it is possible to look at the details of the standard output of GUPIX analysis.



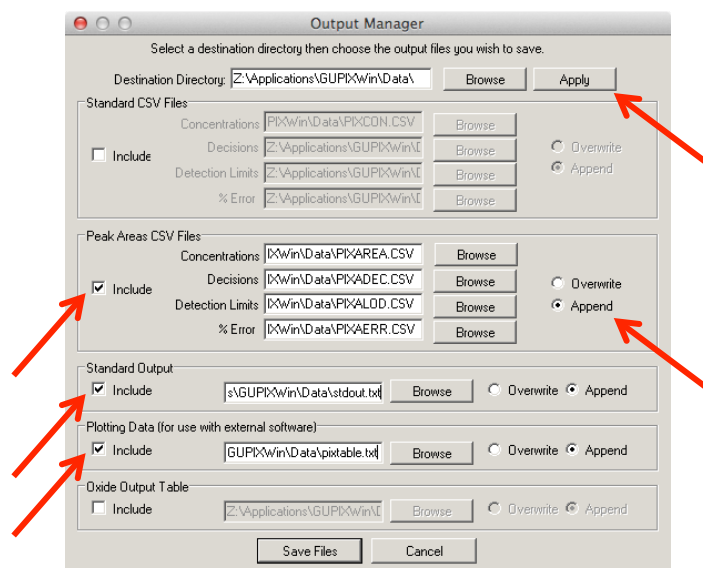
The standard output contains a summary of the general information and user supplied data relevant for peak fitting and background subtraction together with the resulting element peak areas, uncertainties and the areas used to calculate the limit of detection (see Table 2.4).

Statistical error is calculated as squared root of the peak counts, whereas fit error comes from the spectrum fit procedure.

By clicking on the *Output Manager* button it is possible to choose the output files to be saved and in which destination directory. Once the user has browsed the hard disk to choose the destination directory, the path can be automatically applied to all other files to be saved (click *Apply* button). It is suggested to save all the files data in *Append* mode.

The user should create and save the following files, by ticking on the appropriate *Include* box and then by pressing *Save Files*:

- Peak area CSV files:
 - *PIXAREA.CSV*, table of elements and peak areas (in counts), to be used to calculate elemental concentrations;
 - *PIXADDEC.CSV*, table of elements and “decisions” (“Y” = the element is present in amounts more than $1-\sigma$ above the quantization limit, that is $10-\sigma$; “N” = automatic rejection of the presence of that element at minimum detection limit values; or “?” = all other cases, that is the reported value is somewhere between $1-\sigma$ below the MDL value and $1-\sigma$ above the quantization limit);
 - *PIXALOD.CSV*, table of elements and LOD (in counts), to be used to calculate MDL;
 - *PIXAERR.CSV*, table of elements and uncertainties (the maximum between statistical and fit error).
- Standard Output (*STDOUT.TXT*), such as in the previous example or in Table 2.4; it is suggested to include always this file in the output files since the analyst can later on refer to it and check here the complete set of fitting parameters if necessary.
- Plotting Data (*PIXTABLE.TXT*), to be used to produce plots like in Figure 2.7.



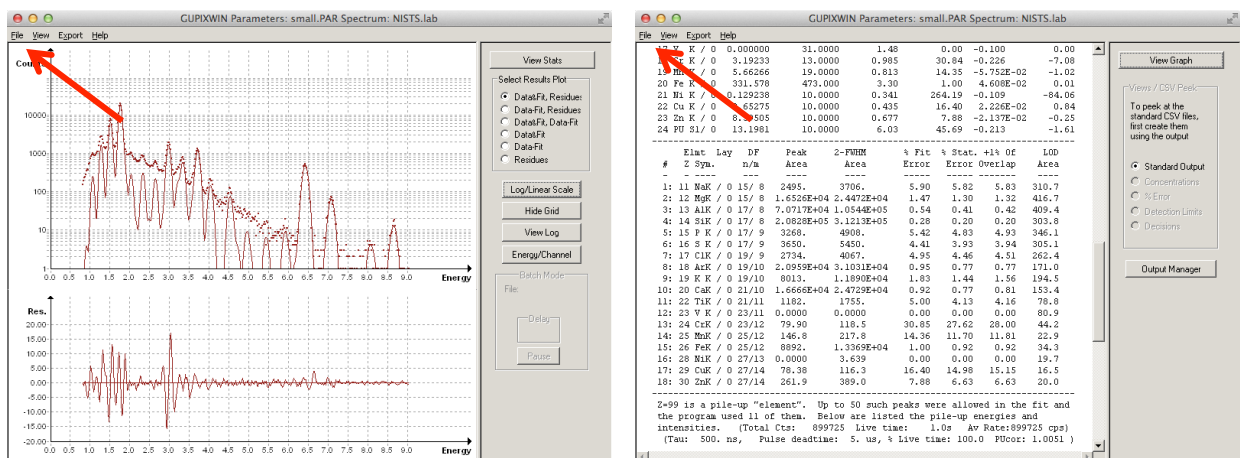
An example of the contents of a *PIXAREA.CSV* file is shown below; please note that parameters such as measurement time, integrated charge and beam current are inserted here just as arbitrary values. Check *Chi*² values.

Type	Filename	Time(s)	Charge(μC)	Ip(nA)	FWHM(eV)	Chi ²	NaK	MgK	AlK	SiK	P K	S K	ClK	ArK	K K	CaK	TiK	V K	CrK	MnK	FeK
Area(counts)	IAEAS001.lab	568	1.000	1.761	133.3	2.527	2515.0	2673.3	9234.4	25187.5	535.0	54630.8	574.6	4437.3	2403.6	13071.0	219.5	101.9	0	10.9	901.4
Area(counts)	IAEAS002.lab	568	1.000	1.761	134.8	4.424	3302.7	7636.7	19026.5	59088.7	1776.3	59550.1	3613.1	4622.6	5797.4	65962.3	637.8	0	60.0	78.2	2419.8
Area(counts)	IAEAS003.lab	568	1.000	1.761	135.2	3.150	1762.7	5663.6	16951.4	50151.8	1050.6	30621.6	2157.9	5296.9	3982.0	24579.4	436.7	28.8	0	41.4	1690.9
Area(counts)	IAEAS004.lab	568	1.000	1.761	136.2	8.338	3755.5	17523.8	40244.4	125976	3242.0	74347.1	10720.1	4441.0	11302.0	106407	1249.5	60.5	21.3	267.9	4929.7
Area(counts)	IAEAS005.lab	568	1.000	1.761	135.1	4.182	1594.9	10780.0	27303.2	85033.4	919.8	21296.7	3464.5	4471.1	4942.8	50350.4	616.3	64.7	40.3	43.9	2540.9
Area(counts)	IAEAS006.lab	568	1.000	1.761	135.3	10.764	3621.3	27196.6	47652.8	157686	4140.3	48126.7	21911.4	3637.7	14623.2	181744	1386.9	12.0	36.5	275.0	5868.1
Area(counts)	IAEAS007.lab	568	1.000	1.761	134.4	4.683	2609.8	8659.3	32414.3	84583.1	757.3	43821.6	5612.0	4135.2	5397.9	26584.2	578.5	0	0	29.1	2212.2
Area(counts)	IAEAS008.lab	568	1.000	1.761	136.8	10.007	4893.9	17678.2	60480.2	161691	2166.9	82366.3	48586.5	4115.0	13875.7	69440.7	1215.4	168.7	0	191.9	4995.5
Area(counts)	IAEAS009.lab	568	1.000	1.761	140.8	1.189	3227.8	965.4	1097.9	1607.0	377.6	29444.2	137.1	6219.3	742.5	1662.9	0	0	0	5.6	93.5
Area(counts)	IAEAS010.lab	568	1.000	1.761	136.1	1.765	3236.4	3735.7	3016.1	12369.0	734.3	40765.1	2236.2	4758.1	2001.2	30843.5	214.7	85.8	0	65.5	668.5
Area(counts)	IAEAS011.lab	568	1.000	1.761	134.5	6.298	2871.5	9800.8	46512.9	122032	1003.4	31031.7	3593.3	7079.1	7318.5	34363.6	789.1	162.6	0	71.4	3218.5
Area(counts)	IAEAS012.lab	568	1.000	1.761	136.4	11.221	4877.6	18311.4	63026.9	174290	2708.0	81286.0	60822.6	4724.9	16365.6	101090	1561.6	122.5	81.1	275.9	5569.7
Area(counts)	IAEAS013.lab	568	1.000	1.761	109.9	0.817	0	0	129.9	434.8	0	0	72.8	5838.3	0	100.5	0	33.3	29.9	0	11.9
Area(counts)	IAEAS014.lab	568	1.000	1.761	136.2	0.319	0	0	73.1	67.5	0	0	7.5	5493.7	15.3	0	0	0	0	0	0
Area(counts)	IAEAS015.lab	568	1.000	1.761	126.5	0.794	0	0	467.1	112.9	2336.7	13.1	760.9	9991.4	95.9	1035.2	51.9	0	0	0	0
Area(counts)	IAEAS016.lab	568	1.000	1.761	131.8	1.687	875.7	737.6	1433.0	5326.6	2376.1	35446.0	878.4	12155.2	1486.8	1503.9	107.2	17.9	7.1	20.0	145.2
Area(counts)	IAEAS017.lab	568	1.000	1.761	137.2	1.875	1361.9	243.9	1197.2	4855.0	2405.3	36038.0	621.9	15831.4	1702.1	1595.4	102.8	87.3	0	0	215.5
Area(counts)	IAEAS018.lab	568	1.000	1.761	127.5	2.865	3203.5	742.9	1873.9	9307.3	4169.9	45604.6	1190.0	20387.0	2253.7	2245.4	148.7	39.0	0	18.1	274.6
Area(counts)	IAEAS019.lab	568	1.000	1.761	141.0	4.237	8503.6	1852.5	1594.6	3719.9	5612.9	80761.7	2051.0	24517.3	3596.1	2622.8	239.6	18.2	58.3	34.6	184.8
Area(counts)	IAEAS020.lab	568	1.000	1.761	134.9	5.059	8248.4	3308.2	11609.0	38621.4	5309.2	95208.6	4189.3	24117.9	7514.3	5034.9	136.9	0	56.6	29.0	1594.8
Area(counts)	IAEAS021.lab	568	1.000	1.761	135.0	4.799	6585.7	2194.5	13689.4	46809.2	4642.5	103203	4411.0	21370.9	6803.2	5666.2	426.7	24.3	0	67.1	1431.7
Area(counts)	IAEAS022.lab	568	1.000	1.761	135.4	9.206	14295.3	10626.0	76036.1	271358	4618.8	56301.4	5284.9	14153.0	24664.4	18602.7	1496.9	127.9	150.8	132.9	8356.7
Area(counts)	IAEAS023.lab	568	1.000	1.761	134.9	11.365	10932.7	9643.3	78241.2	296911	5052.0	81519.1	3887.6	13939.8	30826.4	19669.1	1738.5	197.3	118.5	251.4	10031.8
Area(counts)	IAEAS024.lab	568	1.000	1.761	140.0	7.360	657.0	388.0	600.7	3173.0	3343.7	30488.0	1007.1	33463.7	1360.0	3080.1	134.6	0	7.4	0	156.2

9) Batch analysis

Through a batch analysis the user may set up an automatic process that will fit a sequence of similar spectra using starting from an appropriate saved .PAR file. Before using batch mode it is important that the user runs a few selected individual fits, following all the previous steps, and ensures that all input parameters are correct and that the representative outputs are fully acceptable.

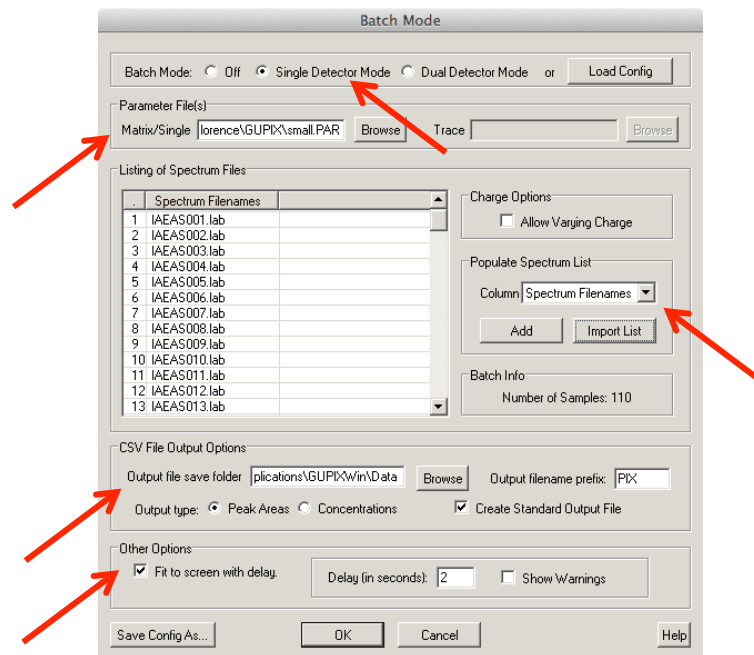
In the *File* menu of the window showing the fitted spectrum or the standard output select the *Do Another Fit* command.



In the *Setup* menu select the *Batch Mode* command. In the *Batch Mode* window the user should choose these suggested options, as shown in the following example:

- *Single detector mode;*

- browse (*Matrix/Single*) to select the aforementioned .PAR file;
- populate the list of the spectrum files to be automatically analysed by importing the list previously written in a file⁴: in the menu *Column* select *Spectrum Filenames* and then press the *Import List* button; otherwise the spectrum files can be added one by one by pressing the *Add* button and browsing to find them;
- browse to select the folder where the output files will be saved (*Output file save folder*);



- choose the output type, by selecting *Peak Areas* and ticking *Create Standard Output File* options. Here is possible to choose the prefix of the output files (defaults is PIX);
- Tick *Fit to screen with delay* option and then select a delay of 2 or 3 seconds (it is the time elapsing from one fit to the other, allowing the user to check that everything is running fine; default value is 10 seconds and the user can keep this default value for the first times). Do not tick the *Show Warnings* option.

The current configuration can be also saved in a *Batch Configuration File* (.BCF extension) in order to be loaded for future analysis. Press *OK*. Then press *OK* in the pop-up window declaring the first file has been successfully loaded.

In the *Gupix* menu select the *Run* command to start the automatic analysis.

⁴ It has to be noted that from the command prompt it is possible to create a file with the list of the .LAB spectra that should be analysed in batch using the following DOS commands. The filename should be limited to 8 characters.

- cd..
- cd..
- cd "folder name"
- dir/s/b *.lab > LIST.TXT

In the given example all the .LAB spectrum files are added to the LIST.TXT file, to be imported in GUPiX.